NEGATIVE CYCLOTRON RESONANCE ABSORPTION

by

Jonathan M. Wachtel

A Dissertation Presented to the Faculty of
the Graduate School of Yale University
in Candidacy for the Degree of
Doctor of Philosophy

1967

Abstract

The kinetic theory of waves in an infinite plasma in a uniform, constant magnetic field predicts that radiation near the cyclotron frequency in a sufficiently non-thermal plasma may grow in time. One effect which can cause such growth or negative cyclotron resonance absorption of radiation which propagates perpendicular to the magnetic field direction is the relativistic energy dependence of the electron's mass. Another is the energy dependence of the electron-atom collision cross section for low energy electrons in a neutral gas background. The cyclotron resonance absorption of microwave energy by monoenergetic electrons which drift through a cavity resonator has been measured in order to verify these predictions. In each case the observed absorption spectra are similar to those calculated in a perturbation theoretical solution of the Boltzmann equation treating the cyclotron resonance interaction between the electron beam and the bounded standing wave fields of the cavity resonator. An experiment which exhibits the radiative response in time of a weakly relativistic, monoenergetic electron ensemble to a short pulse of cyclotron resonance radiation is also described. The radiation calculated in an exact solution of the Boltzmann equation is found to occur in repetitive bursts of diminishing amplitude following the stimulating pulse. Experiment and theory are observed to be in qualitative agreement.

Acknowledgment

This thesis would not be complete without an expression of my indebtedness to Professor Jay L. Hirshfield for four years of personal tutelage and tolerance.

Table of Contents

List of Illustrations

I. Introduction

1. Preliminary Remarks

In the early work on the dispersion and absorption of electromagnetic radiation by dielectrics, the medium was often considered to consist of a collection of fixed, microscopic classical oscillators which reradiated when driven by time varying electromagnetic fields. For some time thereafter classical models were forced out of style by more successful quantum mechanical treatments. The interaction of a system of free charged particles with electromagnetic radiation, a problem which in the low particle density limit is quite accurately described in classical terms, was largely ignored. Recent activity in the field of plasma physics, however, has yielded solutions to a variety of problems regarding the electromagnetic behavior of free charged particle systems. It is to the experimental verification of predictions concerning one class of such interactions that the research to be described here has been directed.

The interactions in this class fall under the general heading of cyclotron resonance phenomena. Cyclotron resonance occurs when a charged particle executing circular (or nearly circular) motion in a constant magnetic field is coupled strongly to radiation fields that oscillate at a frequency near the gyration frequency of the particle motion. Strong coupling can also occur at multiples of the gyration frequency. Each charged particle can be considered as one of many little current oscillators whose

amplitudes and phases as well as positions are distributed according to a distribution function which describes the density of particles in position and momentum space.

The cyclotron resonance phenomena considered in this work pertain only to the coupling between radiation fields and electrons which obey single particle classical dynamics under the influence of a uniform constant magnetic field and the electric and magnetic radiation fields. The medium is tacitly assumed to be uncharged. Physically, a positive charge neutralizing background that does not interact with the radiation fields is imagined to coexist with the electrons.

The distribution function $f(\underline{r},\underline{p},t)$ which specified a statistical knowledge of the electron motion is the normalized electron density in a single particle phase space. It obeys the Boltzmann equation

$$\frac{\partial f}{\partial t} + \underline{v} \cdot \frac{\partial f}{\partial \underline{r}} + e\left(\underline{E} + \frac{\underline{v}}{c} \times \underline{B}\right) \cdot \frac{\partial f}{\partial \underline{p}} = \left(\frac{df}{dt}\right)_{coll.} . \qquad (1)$$

The collisions made by electrons of charge e, mass m, velocity $\underline{v}$, momentum $\underline{p}$ and position $\underline{r}$ are accounted for in the collision term on the right. The fields obey Maxwell's equations.

Exhaustive theoretical studies of the interaction of small amplitude radiation fields with this type of electron plasma have been accomplished in recent years. Methods for classifying the various possible modes of radiation and for obtaining their dispersion relations have been developed. Under certain circumstances the dispersion relation for a particular type of

radiation field predicts that the wave will grow in time. At least two such possibilities exist for radiation near the gyrofrequency of the plasma electrons. The first arises in connection with the anharmonic nature of the motion of a relativistic electron in a magnetic field, and the second is predicted for plasmas consisting of electrons that collide with neutral atoms if the collision frequency is sufficiently energy dependent. Such negative absorption phenomena will only occur in non-equilibrium plasmas.[1,2] The generation of non-equilibrium distribution functions in the experiments which comprise this work has therefore been of fundamental concern.

In this chapter the simultaneous solution of the Boltzmann equation and Maxwell's equations using a method introduced by Bernstein[3] to obtain a general dispersion relation for electromagnetic wave propagation in unbounded plasmas will be summarized. The calculation is well known and has appeared in recent texts on plasma physics.[4,5] The dispersion relation will be specialized to give the growth or damping rates due to the cyclotron resonance interaction.

The original part of this work begins with the second chapter where an experiment which exhibits negative cyclotron resonance absorption by relativistic electrons is described. The collisional effect is studied in the fourth chapter. More precise theories for the relativistic and collisional negative cyclotron resonance absorption phenomena that are experimentally studied are also offered. In the third chapter an experiment which exhibits the radiative response of a monoenergetic, relativistic ensemble of

electrons to a pulse of radiation at cyclotron resonance is described. The experiment could be considered noteworthy because of its illuminating relation with respect to the relativistic negative absorption mechanism and because an exact (non-perturbation) solution of the Boltzmann equation which describes it has been obtained.

2. The Dispersion Relation for Perpendicular Propagation in an Infinite Plasma in a Magnetic Field

In order to introduce these negative cyclotron resonance absorption phenomena the theory for wave propagation in an unbounded, uniform electron plasma in a constant uniform magnetic field will be reviewed. The general dispersion relation for sinusoidal plane wave modes characterized by the wave vector $\underline{k}$ and frequency ω will be specialized for waves which propagate perpendicular to the direction of the magnetic field $\underline{B}_o$. A class of cyclotron resonance interactions that are associated with doppler shifts due to electron motion along $\underline{B}_o$ are thereby eliminated from consideration. These interactions have been studied theoretically by Weibel[6] and Harris.[7] They are not basic to the experiments described here.

Several approximations are made in reducing the dispersion relation to the case of interest. The plasma is considered to be so tenuous that collective effects may be ignored and the damping or growth rates considered to be small. Thus the electrons are independent current oscillators which interact with the fields but not with each other. In the limit of vanishing electron

density the wave reduces to the mode which propagates across $\underline{B}_o$ with its electric field polarized normal to $\underline{B}_o$. The theory will be shown to suggest the existence of the two negative cyclotron resonance absorption phenomena for this mode in low density plasmas. Negative absorption persists even for plasmas whose distribution functions are isotropic in momentum space.

A standard perturbation theory[8] is used to solve the set of equations consisting of the Boltzmann equation and Maxwell's equations. The part of the distribution function unperturbed by the small radiation fields is written $f_o(\underline{p})$ and is assumed to be constant in space and in time. This unperturbed distribution function and the magnet field $\underline{B}_o$ are considered to be zeroth order terms in the perturbation expansion. The first order quantities are the perturbed part of the distribution $f_1(\underline{r},\underline{p},t)$ and the radiation fields $\underline{E}_1(\underline{r},t)$ and $\underline{B}_1(\underline{r},t)$. The total quantities are written

$$f = f_o(\underline{p}) + f_1(\underline{r},\underline{p},t) \ , \tag{2}$$

$$\underline{B} = \underline{B}_o + \underline{B}_1(r,t) \ , \tag{3}$$

$$\underline{E} = \underline{E}_1(\underline{r},t) \ . \tag{4}$$

Since a relativistic effect is to be described the distribution function is written in terms of the momentum instead of velocity. These are related by

$$\underline{p} = \gamma m \underline{v} \tag{5}$$

where

$$\gamma = (1 + p^2/m^2c^2)^{\frac{1}{2}} \quad . \tag{6}$$

The z axis is fixed along the direction of $\underline{B}_o$ and a cylindrical polar coordinate system in momentum space is defined by

$$\underline{p} = p_\perp \cos\varphi\, \hat{e}_x + p_\perp \sin\varphi\, \hat{e}_y + p_\parallel \hat{e}_z \quad . \tag{7}$$

The momentum coordinates $(p_\perp, \varphi, p_\parallel)$ thus specify the magnitude of the momentum in a plane perpendicular to $\underline{B}_o$, its instantaneous direction in that plane and the momentum along $\underline{B}_o$ respectively.

If eqs. (2), (3) and (4) are inserted in the Boltzmann equation and Maxwell's equations and the resulting equations separated according to the order of the terms in the perturbation scheme a linear set of equations is obtained. The collision term of Eq. (1) is treated in the so-called relaxation approximation,

$$\left(\frac{df}{dt}\right)_{coll.} = -\nu_c(f-f_o) = -\nu_c f_1 \tag{8}$$

where the collision frequency ν_c may be velocity dependent. The validity of the ordering procedure is assured if the radiation fields are so small that $|f_1| \ll f_o$. The linear equations

$$\frac{e}{c}(\underline{v} \times \underline{B}_o) \cdot \frac{\partial f_o}{\partial \underline{p}} = 0 \quad , \tag{9}$$

$$\frac{\partial f_1}{\partial t} + \underline{v}\cdot\frac{\partial f_1}{\partial \underline{r}} + \frac{e}{c}(\underline{v} \times \underline{B}_o)\cdot\frac{\partial f_1}{\partial \underline{p}} + e\left(\underline{E}_1 + \frac{\underline{v}}{c} \times \underline{B}_1\right)\cdot\frac{\partial f_o}{\partial \underline{p}} = -\nu_c f_1 , \tag{10}$$

$$c\,\frac{\partial}{\partial \underline{r}} \times \underline{E}_1 = -\frac{\partial \underline{B}_1}{\partial t} \quad , \tag{11}$$

and

$$c \frac{\partial}{\partial \underline{r}} \times \underline{B}_1 = \frac{\partial \underline{E}_1}{\partial t} + 4\pi e n_o \int \underline{v} \, f_1 \, d^3p \tag{12}$$

are obtained. The current in Ampere's law is written directly in terms of the velocity moment of the distribution function with $e < 0$ as the electronic charge and n_o as the number density of the unperturbed electron plasma. The gaussian cgs system of units is employed.

Equation (9) may be rewritten

$$\Omega(p \times \hat{e}_z) \cdot \frac{\partial f_o}{\partial \underline{p}} = 0 \tag{13}$$

noting that $\underline{B}_o = B_o \hat{e}_z$ and defining the cyclotron frequency Ω for electrons of momentum $\underline{p}$ as $eB_o/\gamma mc$. It is a simple exercise involving Eq. (7) to show that Eq. (13) is equivalent to

$$- \Omega \frac{\partial f_o}{\partial \varphi} = 0 \quad . \tag{14}$$

This means that to zeroth order (to which order the radiation fields vanish) there is no preferred direction in the plane perpendicular to $\underline{B}_o$. Consequently the unperturbed distribution function may be written as $f_o(p_\perp, p_\parallel)$.

To progress further, it is noted that $\underline{E}_1$, $\underline{B}_1$ and f_1 possess Fourier-Laplace transforms in the usual sense

$$(\tilde{\underline{E}}_1, \tilde{\underline{B}}_1, \tilde{f}_1) = \int_0^\infty dt \, e^{i\omega t} \int_{-\infty}^{\infty} \frac{d^3r}{(2\pi)^3} \, e^{-i\underline{k}\cdot\underline{r}} \, (\underline{E}_1, \underline{B}_1, f_1) \tag{15}$$

provided that Im $\omega > 0$. The inverse transforms are

$$(\underline{E}_1,\underline{B}_1,f_1) = \int_{-\infty}^{\infty} d^3k\ e^{i\underline{k}\cdot\underline{r}} \int_{-\infty}^{\infty} \frac{d\omega}{2\pi}\ e^{-i\omega t}\ (\tilde{\underline{E}}_1,\tilde{\underline{B}}_1,f_1)\ . \tag{16}$$

If the space Fourier transforms of the initial value fields are written as

$$(\underline{e},\underline{b}) = \int_{-\infty}^{\infty} \frac{d^3r}{(2\pi)^3}\ e^{-i\underline{k}\cdot\underline{r}} \left[\underline{E}_1(t=0),\underline{B}_1(t=0)\right] \tag{17}$$

and if Eqs. (11) and (12) are Fourier-Laplace transformed the results can be combined to give

$$(\omega^2-c^2k^2)\tilde{\underline{E}}_1 + c^2\underline{k}(\underline{k}\cdot\tilde{\underline{E}}_1) = -ic\underline{k}\times\underline{b} + i\omega\underline{e} - 4\pi en_o i\omega \int \underline{v}\ f_1 d^3p \tag{18}$$

This will become a system of three linear equations in the three components of $\tilde{\underline{E}}_1$ when $\tilde{f}_1$ is written as a linear function of $\tilde{\underline{E}}_1$. The coefficients are, in general, functionals of $f_o(\underline{p})$, the unperturbed distribution function. To accomplish this, Eq. (10), the linearized Boltzmann equation is Fourier-Laplace transformed to give

$$\begin{aligned}(-i\omega + i\underline{k}\cdot\underline{v} + \nu_c)\tilde{f}_1 + \frac{e}{c}\ (\underline{v}\times\underline{B}_o)\cdot\frac{\partial\tilde{f}_1}{\partial\underline{p}} \\ + e(\tilde{\underline{E}}_1 + \frac{1}{\omega}\ \underline{v}\times\underline{k}\times\tilde{\underline{E}}_1)\cdot\frac{\partial f_o}{\partial\underline{p}} \\ = g + \frac{e}{i\omega c}\ (\underline{v}\times\underline{b})\cdot\frac{\partial f_o}{\partial\underline{p}}\end{aligned} \tag{19}$$

where the space Fourier transformed initial value of the perturbed part of the distribution function

$$g = \int \frac{d^3r}{(2\pi)^3} e^{-i\underline{k}\cdot\underline{r}} f_1 \ (t=0) \tag{20}$$

has been introduced. The second term in the LHS of Eq. (19) is equal to $-\Omega \ \partial\tilde{f}_1/\partial\underline{p}$. With this substitution Eq. (19) may be rewritten

$$\frac{\partial\tilde{f}_1}{\partial\varphi} - \frac{-i\omega+i\underline{k}\cdot\underline{v}+\nu_c}{\Omega}\tilde{f}_1 = \frac{e}{\Omega}\left(\tilde{\underline{E}}_1 + \frac{1}{\omega}\underline{v}\times\underline{k}\times\tilde{\underline{E}}_1\right)\cdot\frac{\partial f_o}{\partial\underline{p}}$$

$$+ \frac{ie}{\Omega\omega c}(\underline{v}\times\underline{b})\cdot\frac{\partial f_o}{\partial\underline{p}} - \frac{g}{\Omega} \ . \tag{21}$$

In his treatment of wave propagation in a plasma in a magnetic field, Bernstein[3] notes that an integrating factor for this equation is

$$G(\varphi') = \exp\left[\int_{\varphi'}^{\varphi} d\varphi'' \ \frac{-i\omega+i\underline{k}\cdot\underline{v}''+\nu_c}{\Omega}\right] \ . \tag{22}$$

The double prime notation refers only to the angular velocity space coordinate and the notation

$$\underline{v}' = v_\perp \cos\varphi' \ \hat{e}_x + v_\perp \sin\varphi' \ \hat{e}_y + v_\parallel \hat{e}_z \tag{23}$$

will be used again below. With no loss of generality the wave vector $\underline{k}$ can be restricted to the x-z plane. Thus with

$$k = k_\perp \hat{e}_x + k_\parallel \hat{e}_z \tag{24}$$

the integration in Eq. (22) is readily performed to give for the integrating factor

$$G(\varphi') = \exp\left[\frac{-i\omega+ik_{\parallel}v_{\parallel}+\nu_c}{\Omega}(\varphi-\varphi') - \frac{ik_{\perp}v_{\perp}}{\Omega}(\sin\varphi' - \sin\varphi)\right]. \quad (25)$$

The solution of Eq. (21) is

$$\tilde{f}_1 = \frac{1}{\Omega}\int_{-\infty}^{\varphi} d\varphi'\, G(\varphi')\left[e(\tilde{\underline{E}}_1 + \frac{1}{\omega}\underline{v}'\times\underline{k}\times\tilde{\underline{E}}_1)\cdot\frac{\partial f_o}{\partial \underline{p}'}\right.$$

$$\left. + \frac{ie}{\omega c}(\underline{v}'\times\underline{b})\cdot\frac{\partial f_o}{\partial \underline{p}'} - g\right]. \quad (26)$$

For electrons $\Omega < 0$, and since Im $\omega > 0$ the lower limit of integration is chosen to be minus infinity so that the integral converges. The transformed, perturbed distribution function $\tilde{f}_1$ is now inserted into Eq. (18) to obtain

$$(\omega^2-c^2k^2)\tilde{\underline{E}}_1 + c^2\underline{k}(\underline{k}\cdot\tilde{\underline{E}}_1)$$

$$+ \frac{4\pi n_o e^2 i\omega}{\Omega}\int d^3p\, \underline{v}\int_{-\infty}^{\varphi} d\varphi'\, G(\varphi')\left[\tilde{\underline{E}}_1 + \frac{1}{\omega}\underline{v}'\times\underline{k}\times\tilde{\underline{E}}_1\right]\cdot\frac{\partial f_o}{\partial \underline{p}'} = \underline{I} \quad (27)$$

where $\underline{I}$, defined by

$$\underline{I} = i\omega\underline{e} - ic\underline{k}\times\underline{b} + \frac{4\pi n_o e^2 i\omega}{\Omega}\int d^3p\, \underline{v}\int_{-\infty}^{\varphi} d\varphi'\, G(\varphi')\left[g\right.$$

$$\left. - \frac{ie}{\omega c}(\underline{v}'\times\underline{b})\cdot\frac{\partial f_o}{\partial \underline{p}}\right], \quad (28)$$

contains all the initial value terms.

Equation (27) may be expressed in matrix form as

$$\underline{\underline{R}} \cdot \tilde{\underline{E}}_1 = \underline{I} \tag{29}$$

which can be inverted to give

$$\tilde{\underline{E}}_1 = \frac{\underline{\underline{R}}^c \cdot \underline{I}}{\det(\underline{\underline{R}})} \tag{30}$$

where $\underline{\underline{R}}^c$ is the matrix of cofactors of $\underline{\underline{R}}$.
The elements of $\underline{\underline{R}}$ are obtained in terms of $f_o(p_\perp, p_\parallel)$ by performing the angular integrations in the LHS of Eq. (27). The integration over φ' is indicated and that over φ is contained in the momentum space integration $\int d^3p(\ldots) = \int_0^\infty p_\perp dp_\perp \int_{-\infty}^{\infty} dp_\parallel \int_0^{2\pi} d\varphi(\ldots)$. A complicated series involving Bessel functions of argument $k_\perp v_\perp/\Omega$ is generated. For details concerning these integrations the reader is referred to Ref. 5 which contains the treatment being summarized here.

In principle one can insert Eq. (30) into the Fourier-Laplace inversion formula Eq. (16) to obtain an expression for $\underline{E}_1(\underline{r},t)$ for all $t > 0$. However, difficulties involved in such a straightforward approach to the initial value problem are made obvious when the analytic properties of the components of $\underline{\underline{R}}$ and of $\underline{I}$ are examined. Pathological choices of the initial perturbed distribution function or initial fields can lead to a variety of singularities in the numerator of Eq. (30).[9] On the other hand the poles which occur when the denominator vanishes lend themselves to a simple interpretation. The values of ω and of $\underline{k}$ which cause the denominator of Eq. (30) to vanish are considered to define

the normal modes for wave propagation in the plasma medium. This interpretation will be accepted and the remainder of this section will be devoted to finding the interesting solutions of the dispersion relation

$$\det (\underline{\underline{R}}) = 0 \ . \tag{31}$$

At this point it is expedient to specialize to the case of interest. For perpendicular propagation ($k_{\parallel} = 0$) and for isotropic distribution functions $f_o(p_\perp, p_\parallel) = f_o(p)$ where $p = (p_\perp^2 + p_\parallel^2)^{\frac{1}{2}}$ the elements of $\underline{\underline{R}}$ become

$$R_{xx} = -\omega^2 + \frac{2\pi i\omega\omega_p^2}{\Omega_o} \sum_n \int dp_\parallel \int p_\perp^2 dp_\perp \frac{n^2\Omega^3(\partial f_o/\partial p_\perp)J_n^2}{k_\perp^2 v_\perp^2(-i\omega+in\Omega+\nu_c)} \ ,$$

$$R_{xy} = -R_{yx} = \frac{-2\pi\omega\omega_p^2}{\Omega_o} \sum_n \int dp_\parallel \int p_\perp^2 dp_\perp \frac{n\Omega^2(\partial f_o/\partial p_\perp)J_n J_n'}{k_\perp v_\perp(-i\omega+in\Omega+\nu_c)} \ ,$$

$$R_{yy} = -\omega^2 + c^2k_\perp^2 + \frac{2\pi i\omega\omega_p^2}{\Omega_o} \sum_n \int dp_\parallel \int p_\perp^2 dp_\perp \frac{\Omega(\partial f_o/\partial p_\perp)(J_n')^2}{(-i\omega+in\Omega+\nu_c)} \ ,$$

$$R_{zz} = -\omega^2 + c^2k_\perp^2 + \frac{2\pi i\omega\omega_p^2}{\Omega_o} \sum_n \int p_\parallel dp_\parallel \int p_\perp dp_\perp \frac{\Omega(\partial f_o/\partial p_\parallel)(J_n)^2}{(-i\omega+in\Omega+\nu_c)} \ ,$$

and

$$R_{xz} = R_{yz} = R_{zx} = R_{zy} = 0$$

The index n ranges over all integers between plus and minus infinity. The non-relativistic cyclotron frequency is written $\Omega_o = \gamma\Omega$ and $\omega_p = (4\pi n_o e^2/m)^{\frac{1}{2}}$ is the plasma frequency. The primes

upon the Bessel functions indicate a derivative with respect to the argument which in all cases is $k_\perp v_\perp/\Omega$.

A solution of Eq. (31) is sought for frequencies near the cyclotron frequency that describes transverse waves propagating across $\underline{B}_o$. These modes should reduce to the free space limit of electric field polarization normal to $\underline{B}_o$ as the plasma density decreases to zero. For tenuous plasmas ($\omega_p^2 \ll \omega^2$) the non-vanishing off-diagonal elements R_{xy} and R_{yx} may be neglected and in this approximation the solution $R_{yy} = 0$ corresponds to such waves. The mode characterized by $\underline{k} \perp \underline{B}_o \perp \underline{\tilde{E}}_1$ is commonly referred to as the extraordinary wave. The other solutions $R_{xx} = 0$ and $R_{zz} = 0$ correspond to longitudinal plasma oscillations and to a wave whose electric field is oriented along $\underline{B}_o$ respectively.

Another approximation is made by expanding the Bessel functions in powers of the small argument and retaining only lowest order terms. The argument $k_\perp v_\perp/\Omega$ is of the order of the ratio of the radius of the cyclotron orbit of an electron to the wavelength of the radiation. Only the $n = \pm 1$ terms in the sum will be zeroth order in $k_\perp v_\perp/\Omega$. Therefore the interaction between the fields and the electrons will be strongest near the cyclotron frequency and weak at cyclotron harmonic frequencies. Cyclotron harmonic interactions originate with the anharmonic nature of the force on an electron due to the finite extent of its cyclotron orbit in a sinusoidally space dependent radiation field. The small argument $k_\perp v_\perp/\Omega$ is also of the order of $v_\perp/c$ for waves near the cyclotron frequency Ω. Thus for $\omega \sim -\Omega$ only the $n = -1$ term

need be considered and the dispersion relation for the extraordinary wave in an isotropic, tenuous, weakly relativistic electron plasma is simply

$$\omega^2 - c^2k_\perp^2 + \frac{\pi\omega\omega_p^2}{2\Omega_o}\int_{-\infty}^{\infty} dp_\parallel \int_0^\infty p_\perp^2 dp_\perp \frac{\Omega\, \partial f_o/\partial p_\perp}{\omega + \Omega + i\nu_c} = 0 \ . \qquad (32)$$

It is noted that the last term in the LHS is smaller than ω^2 for consistency with the neglect of R_{xy} and R_{yx} which amounted to ignoring collective polarization effects in the medium. The picture of the medium as being composed of independent microscopic current oscillators is thereby obtained.

Since the distribution function $f_o(p_\perp, p_\parallel)$ has been assumed isotropic and since the cyclotron frequency Ω or the collision frequency depends only upon the magnitude p of the momentum, Eq. (32) will be written in terms of p alone. Introducing new variables of integration (p,θ) via $p_\perp = p\cos\theta$ and $p_\parallel = p\sin\theta$, and noting that

$$\partial f_o/\partial p_\perp = (p_\perp/p)\, \partial f_o/\partial p$$

Eq. (32) becomes

$$\omega^2 - c^2k_\perp^2 + \frac{\pi\omega\omega_p^2}{2\Omega_o}\int_{-\pi/2}^{\pi/2} \cos^3\theta\, d\theta \int dp\, p^3 \frac{\Omega\, \partial f_o/\partial p}{\omega + \Omega + i\nu_c} = 0 \qquad (33)$$

or

$$\omega^2 - c^2k_\perp^2 + \frac{2\pi\omega\omega_p^2}{3\Omega_o}\int_0^\infty dp\, p^3 \frac{\Omega\, \partial f_o/\partial p}{\omega + \Omega + i\nu_c} = 0 \ . \qquad (34)$$

3. Negative Cyclotron Resonance Absorption in an Infinite Plasma

The dispersion relation can be solved approximately for the small growth or damping constant Im ω; but before a solution is indicated the validity of the dispersion relation for negative values of Im ω must be established. It will be remembered that the Laplace transforms were defined only for positive Im ω. The dispersion relation must, therefore, be analytically continued into the lower half ω-plane in order to define modes that decay in time. The necessity for the analytic continuation of the dispersion relation was first pointed out by Landau[10] for the case of damped electrostatic waves in a collisionless plasma. Enlightened discussions of this topic appear in more recent publications.[11]

The dispersion relations for the normal modes of electromagnetic wave propagation in collisionless plasmas are difficult to interpret because the integrals involved have singular integrands. Eq. (34) is an example if ν_c is set equal to zero. At some particular momentum p the electron gyrofrequency and the wave frequency are equal, and for undamped waves the denominator of the integrand vanishes. The procedure introduced by Landau is to interpret the integral in the Cauchy principal value sense for vanishingly small positive Im ω. The analytic continuation is then straightforward. A dispersion relation is chosen for Im $\omega < 0$ that converges to the same expression as Im ω goes to zero from below. However, the complicated dependence of the cyclotron frequency on momentum makes the mathematics involved in the present situation more difficult. The approach to be used

here will be to retain the collision frequency ν_c in the dispersion relation whence for $|\text{Im } \omega| < \nu_c$ the integrand in Eq. (34) is non-singular for all real p. Thus for small Im ω the dispersion relation of Eq. (34) is its own analytic continuation into the lower half ω-plane and damped modes are well defined.

As a first approximation to the solution of the dispersion relation Eq. (34) the effect of the plasma is neglected and the free space result $\omega = ck_\perp$ is obtained. It is the zeroth order term in an expansion of the dispersion relation in powers of ω_p^2 as may be verified by the following procedure. Equation (34) is abbreviated $D(\omega,k_\perp) = 0$ and is expanded about $\omega = ck_\perp$ to obtain

$$D(\omega,k_\perp) \simeq D(ck_\perp,k_\perp) + \frac{\partial D}{\partial \omega}\bigg|_{\omega=ck_\perp} (\omega - ck_\perp) = 0 \qquad (35)$$

or

$$(\omega - ck_\perp) = \frac{-D(ck_\perp,k_\perp)}{\dfrac{\partial D}{\partial \omega}\bigg|_{\omega=ck_\perp}} \quad . \qquad (36)$$

Inserting $D(\omega,k_\perp)$ from Eq. (34) into Eq. (36) and extracting the imaginary part gives for the growth or damping rate correct to first order in ω_p^2

$$\text{Im } \omega \simeq -\frac{\pi\omega_p^2}{3\Omega_o} \text{Im} \int_o^\infty dp\ p^3 \frac{\Omega\ \partial f_o/\partial p}{ck_\perp + \Omega + i\nu_c} \quad . \qquad (37)$$

An alternative expression that follows after an integration by

parts is

$$\text{Im } \omega \simeq \frac{\pi\omega_p^2}{3\Omega_o} \text{ Im} \int_o^\infty dp\ f_o(p)\ \frac{\partial}{\partial p}\left[\frac{p^3\Omega}{ck_\perp+\Omega+i\nu_c}\right] . \qquad (38)$$

For low energy non-relativistic electrons which suffer collisions at the same frequency Eq. (38) can be integrated trivially for arbitrary $f_o(p)$ to give the Lorentzian shaped absorption spectrum. In this case the wave is always damped. On the other hand if the collision frequency depends upon the energy of the electrons the form of the distribution function is crucial and growth is even possible. A more detailed analysis that reveals growth for sharply peaked distribution functions is offered later in this chapter.

For distribution functions which represent a broad range of relativistic momenta Eq. (37) may be used to obtain a simple result for Im ω. The collision frequency is considered to be a constant. If the wave frequency $ck_\perp$ and the non-relativistic cyclotron frequency Ω_o are fixed, the integrand may contain a sharply peaked resonance at some particular momentum p. An expression for Im ω equivalent to Eq. (37) is

$$\text{Im } \omega \simeq \frac{\pi\omega_p^2}{3\Omega_o} \int_o^\infty dp\ p^3\ \frac{\partial f_o}{\partial p}\ \Omega\ \frac{\nu_c}{(ck_\perp+\Omega)^2 + \nu_c^2} . \qquad (39)$$

If $f_o(p)$ is broad with respect to the width in p of $[(ck_\perp+\Omega)^2 + \nu_c^2]^{-1}$, then Eq. (39) may be symbolically written

$$\text{Im } \omega \simeq \frac{\pi\omega_p^2}{3\Omega_o} \int_o^\infty dp\ p^3 \frac{\partial f_o}{\partial p}\ \Omega\ \delta(ck_\perp+\Omega) \quad . \tag{40}$$

Physically this states that only a narrow range of momenta satisfy the cyclotron resonance condition and that those resonant electrons cause growth or damping of the wave according to the sign of the slope of the distribution function at that value of momentum. Clearly the wave is damped if $\partial f_o/\partial p$ is negative and it grows if $\partial f_o/\partial p$ is positive. This is the classical analog of the quantum mechanical requirement that higher energy states be overpopulated for maser action to occur.

In the following sections the absorption spectra for narrow distribution functions will be discussed.

4. Negative Cyclotron Resonance Absorption by Weakly Relativistic, Monoenergetic Electrons

In anticipation of the fact that the experiments to be described later have been performed upon monoenergetic electron beams Eq. (38) will be evaluated for the monoenergetic, isotropic distribution function

$$f_o(p_\perp, p_\parallel) = \frac{1}{4\pi P^2}\ \delta(p-P) \quad . \tag{41}$$

An electron beam is not, however,, isotropic in momentum space. Albeit, the absorption line shapes observed in the experiments will subsequently be shown to be but slightly modified by the anisotropic nature of the unperturbed distribution function.

Recalling the transformation $p_\perp = p \cos\theta$ and $p_\parallel = p \sin\theta$ and noting that $p = (p_\perp^2 + p_\parallel^2)^{\frac{1}{2}}$ it is an easy matter to show that the distribution function of Eq. (41) is correctly normalized. The calculation follows:

$$\int_0^{2\pi} d\varphi \int_0^{\infty} p_\perp dp_\perp \int_{-\infty}^{\infty} dp_\parallel \frac{1}{4\pi P^2} \delta(p-P)$$

$$= 2\pi \int_{-\pi/2}^{\pi/2} \cos\theta \, d\theta \int_0^{\infty} p^2 dp \frac{1}{4\pi P^2} \delta(p-P) = 1 \, .$$

Inserting this delta function distribution into Eq. (38) and integrating one obtains for the damping or growth constant in a weakly relativistic plasma

$$\text{Im } \omega \simeq \frac{\omega_p^2}{12} \text{Im} \frac{1}{P^2} \frac{\partial}{\partial P} \left[\frac{P^3(1 - P^2/2m^2c^2)}{ck_\perp + \Omega_o(1-P^2/2m^2c^2) + i\nu_c} \right] \tag{42}$$

The approximation $\Omega \simeq \Omega_o(1 - p^2/2m^2c^2)$ has been used. Differentiation and extraction of the imaginary part leads to the expression

$$\text{Im } \omega \simeq - \frac{\omega_p^2}{12\nu_c} \left[\frac{3-5\varepsilon/mc^2}{1 + \delta^2} + \frac{4\beta\delta}{(1+\delta^2)^2} \right] \tag{43}$$

where $\varepsilon = P^2/2m$ is the non-relativistic expression for the energy. The frequency deviation from exact cyclotron resonance in units of the collision frequency is

$$\delta = (-\Omega_o/\nu_c)(1+ck_\perp/\Omega_o - \varepsilon/mc^2) \text{ and } \beta = (-\Omega_o/\nu_c)(\varepsilon/mc^2).$$

Terms have been kept to first order in ε/mc^2. For $\nu_c \ll \Omega_o$ in a weakly relativistic plasma the factor $5\varepsilon/mc^2$ in Eq. (43) is but a small correction. Neglecting it gives the cyclotron resonance absorption line shape in terms of the frequency variable δ and the parameter β alone. Thus Eq. (43) becomes

$$-\frac{4\nu_c}{\omega_p^2}\,\mathrm{Im}\,\omega \simeq \frac{1}{1+\delta^2} + \frac{4/3\,\beta\delta}{(1+\delta^2)^2} \quad . \tag{44}$$

This result is plotted in Fig. 1. Negative absorption is observed to occur for magnetic field strengths lower than the cyclotron resonance value if $\beta > 3/2$. The quantity β is a measure of the amount of relativistic phase focusing that can occur in the momentum space plane normal to $\underline{B}_o$ in a collision time ν_c^{-1}. This phase focusing is a result of the energy dependence of the electron's gyrofrequencies. It produces currents associated with the second term in the RHS of Eq. (44) which add to or cancel those associated with the first (Lorentzian shaped) term to give respectively enhanced absorption or negative absorption of the wave. The predicted absorption lineshape in Fig. 1 will be compared with experimental results. An experiment which explicitly illustrates the cyclotron orbital phase focusing effect will also be described.

5. Negative Cyclotron Resonance Absorption by Slow, Monoenergetic Electrons Due to Collisions

A class of negative absorption phenomena which owe their existence to the energy dependence of electron-neutral atom collision cross sections have often been discussed in the published

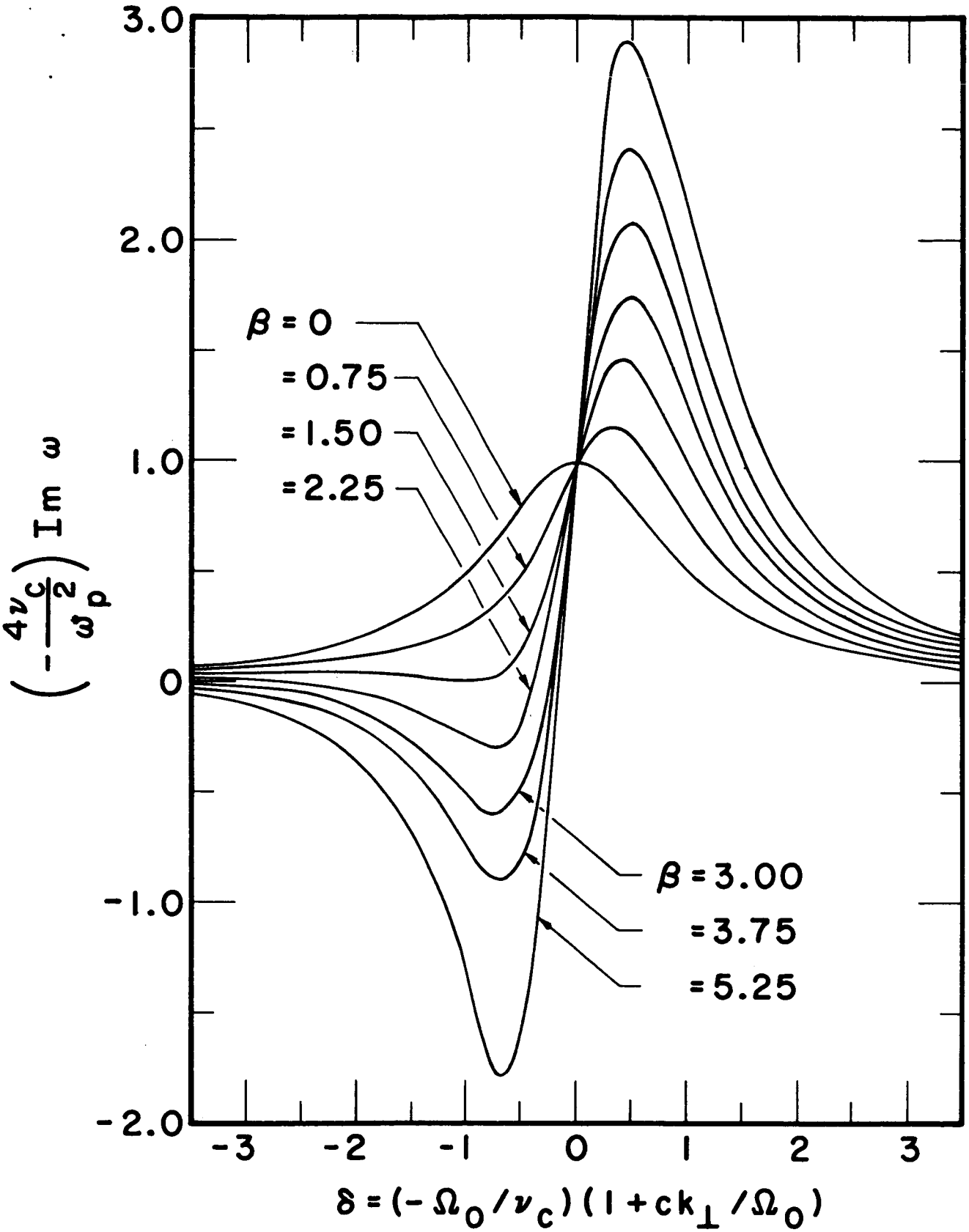

Fig. 1. Cyclotron resonance absorption spectra for weakly relativistic monoenergetic electrons for various values of $\beta=(-\Omega_0/\nu_c)(\varepsilon/mc^2)$.

literature.[12] For the case of cyclotron resonance no definitive experiments have been performed although some suggestive results have been obtained.[13] The effect of collisions upon cyclotron resonance absorption is particularly simple to analyze if the relaxational approximation is applied using an energy dependent collision frequency.[14] In this research experimental absorption line shapes which resemble those predicted in the simple theoretical result below have been obtained.

The most interesting cross section behavior occurs at energies of a few eV. Atoms exhibiting the Ramsauer effect[15] are a case in point. The growth or damping rate for monoenergetic isotropic distribution functions given in Eq. (42) may be applied if the relativistic corrections are neglected and if the collision frequency is considered to be a function of momentum. If $\nu_c(p)$ is a smoothly varying function in the neighborhood of the electron momentum P one can write

$$\text{Im } \omega = \frac{\omega_p^2}{12} \text{ Im } \frac{1}{P^2} \frac{\partial}{\partial P} \left[\frac{P^3}{ck_\perp + \Omega_o + i\nu_c(P)} \right] . \tag{45}$$

After differentiation and extraction of the imaginary part the result

$$-\frac{4\nu_c}{\omega_p^2} \text{ Im } \omega = \frac{1 + \alpha/3}{1 + \delta^2} - \frac{2\alpha/3}{(1+\delta^2)^2} \tag{46}$$

is obtained. The normalized frequency deviation from exact cyclotron resonance is $\delta = (-\Omega_o/\nu_c)(1+ck_\perp/\Omega_o)$ where ν_c is the collision frequency for electrons of momentum P. The parameter

$\alpha = P\nu_c'(P)/\nu_c(P)$ is a measure of the slope of the collision frequency at momentum P. It determines the amount of selective phase randomization that occurs to produced enhanced or negative absorption. The RHS of Eq. (46) is plotted as a function of δ in Fig. 2 for several positive values of the parameter α. Negative absorption at cyclotron resonance is predicted for $\alpha > 3$. Negative absorption can also occur for $\alpha < -3$ at either side of cyclotron resonance. This case is illustrated in Fig. 3.

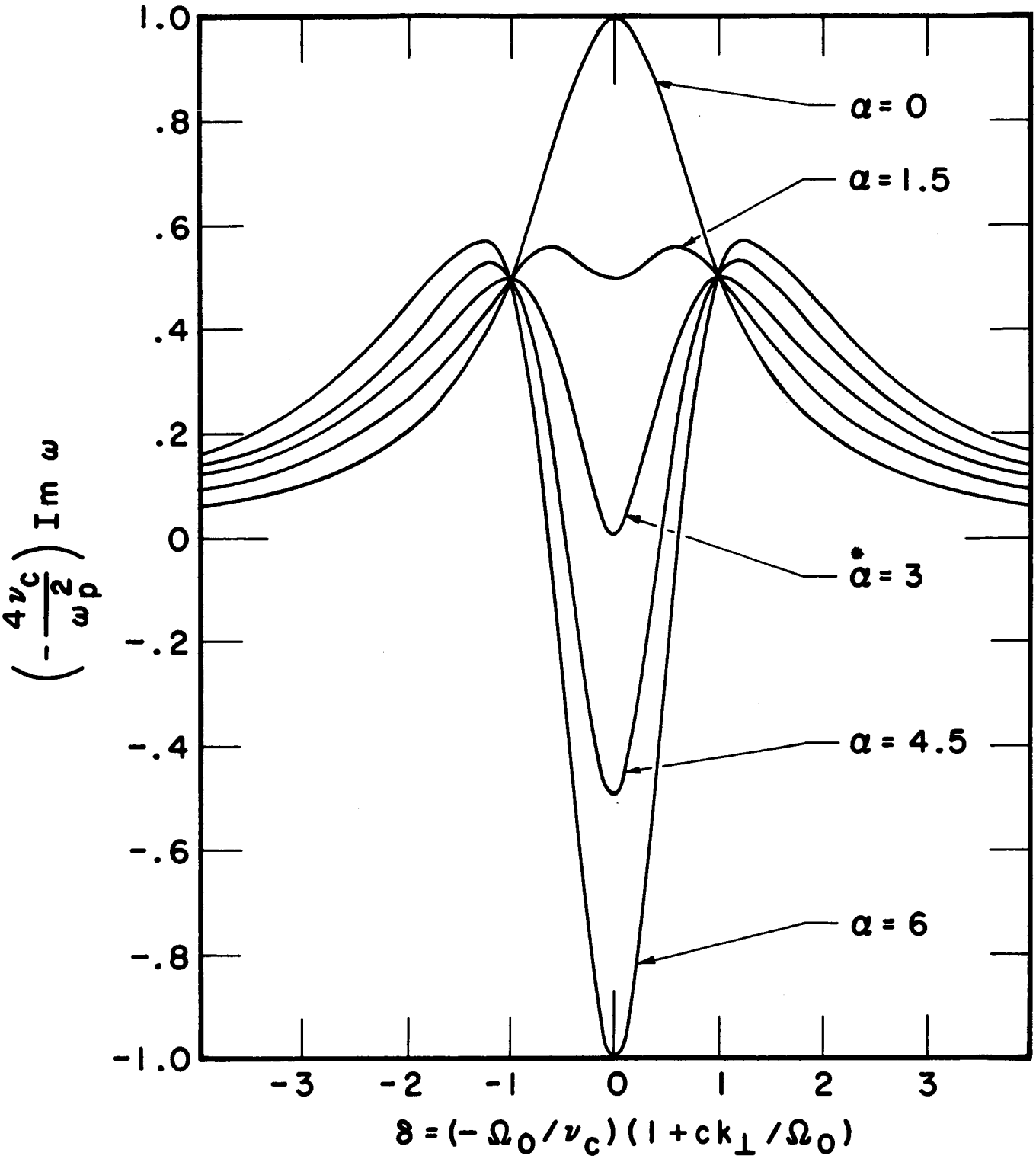

Fig. 2. Cyclotron resonance absorption spectra for non-relativistic electrons in a neutral gas background for various positive values of $\alpha = P\nu_c'(P)/\nu_c(P)$.

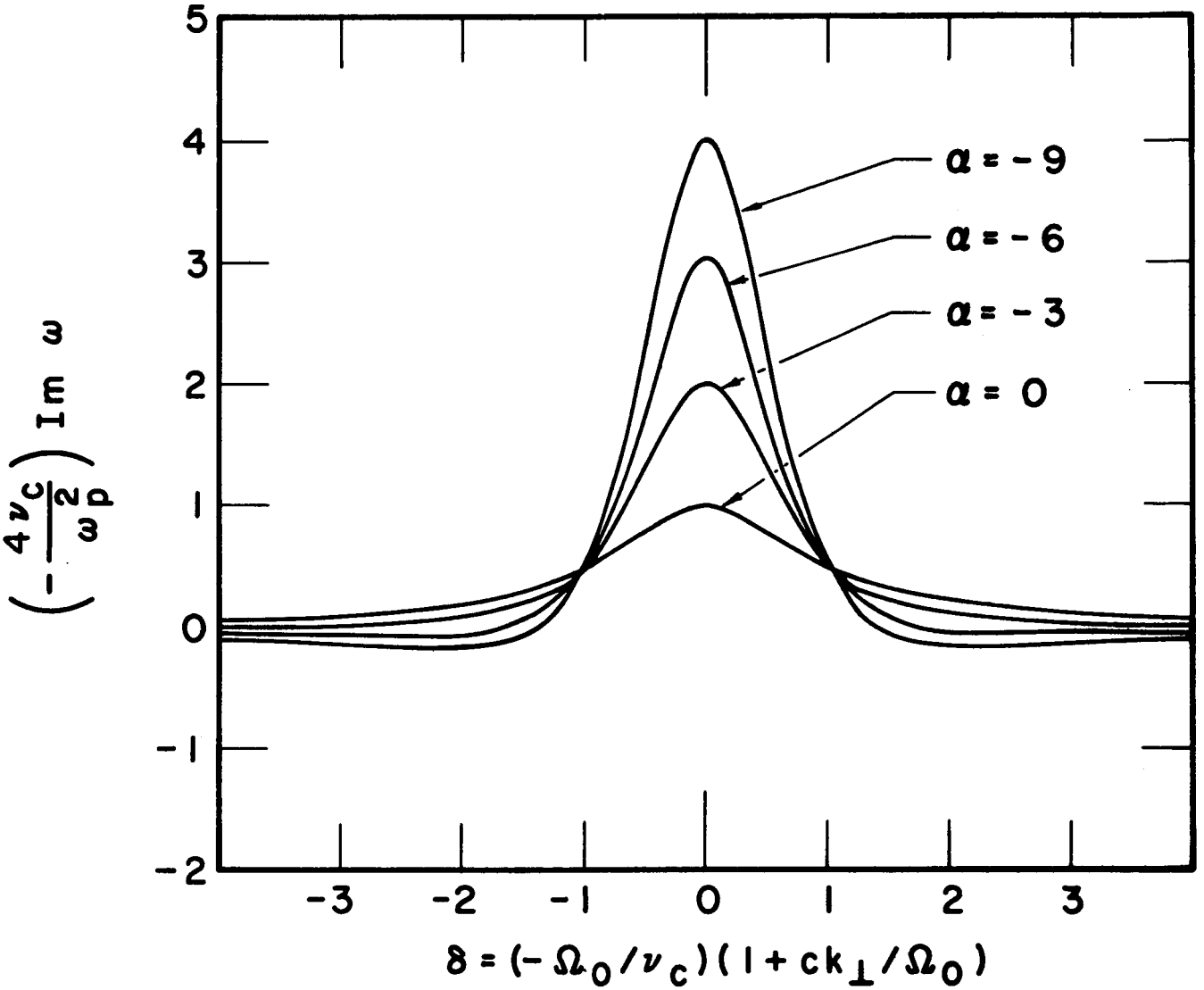

Fig. 3. Cyclotron resonance absorption spectra for non-relativistic electrons in a neutral gas background for various negative values of $\alpha = P\nu_c'(P)/\nu_c(P)$.

II. Negative Cyclotron Resonance Absorption by a Weakly Relativistic Electron Beam

1. Formulation of the Experimental Method

Although a general theoretical treatment of wave propagation in a hot plasma is most easily accomplished by an infinite plane wave normal mode analysis, certain problems are encountered if a direct experimental verification of such a theory is attempted. Experimental cyclotron resonance absorption spectra could be expected to resemble the results in Figures 1, 2 or 3 only if the dimensions of the interaction region were many wavelengths long. If, for example, a reasonable cyclotron resonance magnetic field strength is of the order of 2000 gauss, cyclotron resonance occurs at approximately 6000 Mc/sec. The free space wavelength $2\pi/k_{\perp}$ would be 5 cm. An apparatus whose dimensions are several meters would be necessary. Alternatively higher magnetic fields may be contemplated but the difficulty of obtaining stable monochromatic radiation sources at the correspondingly higher cyclotron frequencies becomes an annoying factor. Practical considerations seem to limit the choice of frequency to the centimeter wavelength microwave range.

If one were able to generate homogeneous magnetic fields of the order of a few kilogauss in large regions filled with a suitable electron plasma, one would still be faced with the problem of maintaining a propagating electromagnetic wave. The electromagnet itself would be the primary obstacle. A direct

laboratory scale test of the results obtained from a free space plane wave dispersion relation is clearly not possible.

A logical compromise would be to measure the spatial growth or decay of bounded plane waves in a plasma filled waveguide whose axis lies in a direction perpendicular to the magnetic field. Practical laboratory dimensions would limit the interaction length to a few wavelengths and since the growth or damping rates must be small for the theoretical predictions of the last chapter to hold, the effect might well be immeasureably small.

Without pursuing any further the objections to experiments on propagating waves, the experimental technique used in this work will be introduced. The electron gas is allowed to drift along $\underline{B}_o$ through the bounded standing wave environment of a microwave cavity. The cavity is excited at the resonant frequency of a mode chosen so that its electric field lies in a plane perpendicular to $\underline{B}_o$. The electrons interact with the cavity fields and the absorption of field energy is measured using a conventional microwave spectrometer as the uniform magnetic field is swept through cyclotron resonance.

The electrons must interact with the cavity fields for a significant number of periods of oscillation. The time interval that they do spend in the cavity plays the role of the relaxation time ν_c^{-1} found in the plane wave calculation. It must be large for negative absorption to occur. Thus the interaction of the cavity fields with electrons which traverse the cavity in ν_c^{-1} seconds and which suffer no collisions is qualitatively similar

to the interaction described in the unbounded plane wave analysis for electrons which suffer collisions every ν_c^{-1} seconds.

With the exception of possible transit time effects the absorption line shape of Fig. 1 should be experimentally observed. This conclusion is supported by the experimental results and by a calculation which treats the problem of energy absorption by electrons in the standing wave environment of a cavity.

The remainder of this chapter is devoted to the relativistic effect. The experiment will be described in detail and a more precise theory for the experimental configuration used than the self consistent field, plane wave analysis will be offered.

2. The Structure and Operation of the Apparatus

The objective of the experimental design was to obtain a weakly relativistic electron beam which would drift slowly in the direction of a uniform magnetic field while passing through an evacuated microwave cavity resonator. All but a small fraction of the electrons' energy would be associated with rotational motion about magnetic field lines. The cavity was designed to be coupled to a microwave spectrometer which would measure the cyclotron resonance absorption of microwave field energy in the cavity by the electrons.

A device known as a "magnetic corkscrew"[16] was used to obtain the desired distribution of electron momenta from an electron beam. This device transforms momentum of charged particle motion along a magnetic field into momentum transverse to the field. It has been used in experiments on plasma confinement with moderate

success.[17,18] The magnetic corkscrew is constructed by loosely winding a few turns of wire about a tube which contains the electron beam. A return winding placed between the turns of the first carries the current of the first back to its source. Since the solenoidal currents cancel, no magnetic field parallel to the axis of the device (at its axis) is generated. A weak transverse magnetic field is, however, generated because the turns are widely spaced. The direction of this field rotates periodically along the axis of the device which is immersed in a uniform magnetic field with its axis parallel to it. With the turns of the corkscrew winding spaced so that the pitch of the weak transverse magnetic field equals the pitch of the helical electron orbit for a given axial velocity in the strong axial field, the transverse energy of the electron will increase at the expense of its energy associated with motion parallel to the axial field. No more than a fraction of the total energy of an axially streaming electron beam may be transformed into energy of rotation by a weak corkscrew magnetic field unless the pitch of the corkscrew winding is reduced along the tube to compensate for the reduction in axial velocity. In the corkscrew device used no such compensation was attempted.

For electrons which enter the corkscrew with no transverse velocity $v_\perp$, and which remain in exact helical resonance with the perturbing corkscrew field $b_\perp$, it is shown in Ref. 17 that the transverse velocity is always perpendicular to the transverse field. The equation of motion

$$\frac{d\underline{v}}{dt} = \frac{e}{\gamma mc}\,\underline{v} \times \underline{B} \tag{47}$$

may be integrated to give the result

$$v_{\perp} = \frac{e}{\gamma mc}\int b_{\perp}(z)\,dz \tag{48}$$

The integration is along the axis of the corkscrew which coincides with the direction of the axial part of $\underline{B}$. The corkscrew used in the experiments was designed for 5 keV electrons. It was constructed with a pitch of 5.7 cm per turn and had four turns. The axial magnetic field for which 5 keV, axially streaming electrons have the same pitch is 275 gauss. According to Eq. (48), $b_{\perp} \simeq 2.6$ gauss is necessary for ten percent of the total energy to become rotational energy. The electrons emerge from the magnetic corkscrew with nearly the same axial velocity as that with which they entered.

Referring to the pictorial rendition of the apparatus in Fig. 4, the electrons are observed to enter a second region which contains a very uniform axial magnetic field. Its intensity is approximately 2070 gauss for cyclotron resonance at 5800 Mc/sec and near the axis of symmetry of the configuration it is uniform to within ±0.2 gauss. This region is separated from the magnetic corkscrew region by a one inch thick cold rolled steel plate. The tube whose outer diameter is 1.05 inches and wall thickness is 1/16 inch passes through a 2 inch diameter hole bored in the steel plate. The tube and the hole in the plate are coaxial with pancake type solenoid windings which support the axial magnetic

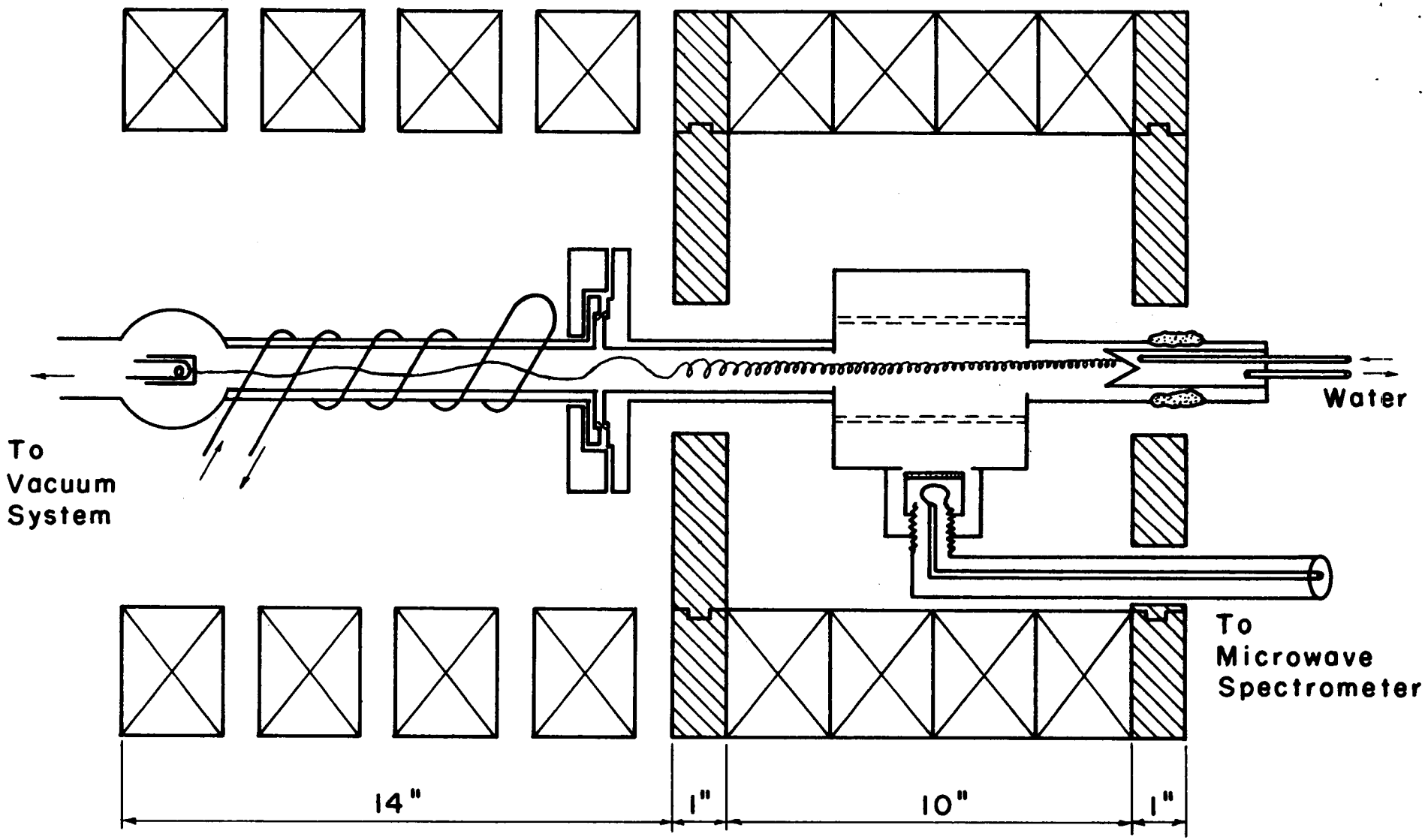

Fig. 4. Apparatus for measuring the cyclotron resonance absorption of weakly relativistic electrons.

fields. A similar plate at the far end of the cyclotron resonance field region helps to maintain the field uniformity.

The electrons which emerge from the corkscrew magnetic field region execute helical motion about converging magnetic field lines as they pass through the hole in the steel plate. The field convergence has the effect of further increasing the rotational kinetic energy of the electrons at the expense of their energy of parallel motion. In fact, if the electrons possess a large enough kinetic energy of rotation before they enter the increasing field region they are turned around by the converging field. This is the well known magnetic mirror effect although in this experiment the effect is not entirely due to the adiabatic invariance of the orbital magnetic moment. Only near the end of the magnetic mirror region where the electrons, having lost most of their parallel energy, execute many periods of cyclotron rotation as they traverse a length over which the field increases moderately is the familiar adiabatic condition an accurate description.[19] The dynamics for the case of a sharply increasing (non-adiabatic) magnetic mirror is somewhat complicated and has been treated elsewhere.[20]

The electrons which enter the cyclotron resonance region between the steel plates drift slowly in the axial direction. The small fraction of their total energy of 5 keV that was associated with the axial drift was varied by changing the current in the corkscrew winding. A current of 15 amperes was sufficient to bring the drift velocity to zero at some point in the magnetic mirror region thus cutting off the beam entirely.

Midway between the steel plates the electrons drift through a microwave cavity resonant at 5800 Mc/sec in the TE011 mode. The axis of the cavity was parallel to the tube axis and to $\underline{B}_o$ so that the electric field of the cavity mode was perpendicular to $\underline{B}_o$. Rods were placed in the cavity which were displaced from and parallel to its axis. These served to suppress the TM111 mode which is frequency degenerate with the desired TE011 mode. The cavity formed part of the vacuum chamber itself and coupling was accomplished via a microwave transparent ceramic vacuum window. An inductive loop coupled the cavity fields to the field of a coaxial transmission line that passed through a second but smaller (3/4 inch diameter) hole in the second steel plate. The electron current was collected and returned to the 5 keV potential source by an insulated water cooled collector.

The tube was constructed entirely of type 304 non-magnetic stainless steel except for the cavity whose walls were of OFHC copper. It was sectioned and joined utilizing commercially available vacuum flanges which form seals by compressing copper gaskets. All structural joints were either brazed in vacuum or welded in an inert gas atmosphere in accordance with recommended high vacuum procedures.[21]

A chamber placed immediately before the magnetic corkscrew housed the electron gun. The cathode used was a barium compound impregnated, circular tungsten disc mounted in a molybdenum sleeve. The disc surface faced the magnetic corkscrew and was concentric with the tube. The cathode and heater (which rested in the molybdenum sleeve behind the emitting surface) were supported by

wires which passed through a vacuum flange via ceramic insulators. The flange was sealed to the mating chamber flange surface by compressing an annealed gold wire (.025 inch) "O" ring. The cathode to which one heater lead was connected floated at a negative potential with respect to the grounded tube body. The heater current was reduced from its maximum of 10 amperes to afford an independent control over the total current in the tube.

The tube was connected at the electron gun end to a high vacuum system which maintained a pressure of 2×10^{-9} mm Hg after baking for 24 hours at 400°C. The vacuum system was mounted on a heavy steel cart which rolled on tracks that were parallel to the axis of the solenoid magnet. The tube was thus rolled into the magnet which had a seven inch bore. The cavity, however, could not pass through the two inch diameter holes bored in the steel plates. Consequently the plates were constructed with a seven inch wide removable section. The top half of the removable section could be lifted up and out like a gate in a castle wall at the head of a drawbridge. The bottom semi-circular half could then be rotated around the tube and lifted out. Some dimensions are indicated in Fig. 4 although the drawing is not to scale. It will also be noted that only two of the four turns of the corkscrew winding are indicated.

3. The Microwave Spectrometer

The resonant frequency of the cavity is found by tuning the stabilized klystron used as the source of microwave power until the power reflected at the single coupling port is minimized.

If, however, the cavity contains electrons gyrating in a magnetic field for which the cyclotron frequency is near the resonant frequency of the driven cavity mode, then the response of the system is more complicated because the electron gas is highly dispersive and absorptive for frequencies near cyclotron resonance.

Fortunately much attention has been given to the problem of a simple resonant circuit which interacts with a collection of absorbing oscillators via its own oscillating fields. The problem is central to the interpretation of most experiments in the areas of radio frequency and microwave spectroscopy. In practice it consists of interpreting the measured change in the response of a resonator excited at a fixed frequency (near its own resonance) as a magnetic field is varied in the neighborhood of the value which equalizes the excitation frequency and the frequency of the classical or quantum oscillators which constitute the absorbing medium. In their early work on nuclear magnetic resonance at radio frequencies, Bloembergen, Purcell and Pound[22] showed how the response of an RLC circuit in which the inductor contained the magnetically active sample gave the bulk absorption and dispersion of the sample directly. Their methods are applicable when the fields of the empty resonator are but slightly perturbed by the sample. In subsequent years their techniques have been extended to microwave frequencies by many workers.

The particular type of microwave spectrometer used in these experiments was first described by Gordon.[23] It utilized a reflection type cavity and eliminated the necessity for a reference signal waveguide arm that had been used in the usual microwave

bridge circuit. A signal at the resonant frequency of the empty cavity was partially reflected at the cavity coupling hole. This reflected signal furnished a reference phase with respect to which small changes in the cavity reflection that occurred when the magnetic field was tuned to cyclotron resonance were measured. If the change in the amount of signal reflected due to the cyclotron resonance absorption of the cavity fields by the electrons was much smaller than the signal reflected due to the under-or over-coupling necessary to provide the reference signal, then the total reflected signal measured on a power sensitive detector, as a function of magnetic field, was proportional to the energy absorbed by the electrons. The cyclotron resonance absorption spectrum could thus be exhibited directly.

The incident and reflected signals were separated by a waveguide "magic T" as indicated in the schematic representation of the apparatus in Fig. 5. The detector used was a microwave crystal rectifier in a waveguide mount. The voltage generated at the crystal was displayed on an oscilloscope whose horizontal trace was swept in synchronism with the cyclotron resonance magnetic field. Isolators used to eliminate unwanted reflected signals, attenuators used to vary the field strength of the driven cavity oscillation and microwave power measuring equipment are not shown in Fig. 5.

4. The Measured Absorption and Oscillation Spectra

The photograph of Fig. 6a shows the absorption spectrum displayed on the oscilloscope when the magnetic B_o was swept at

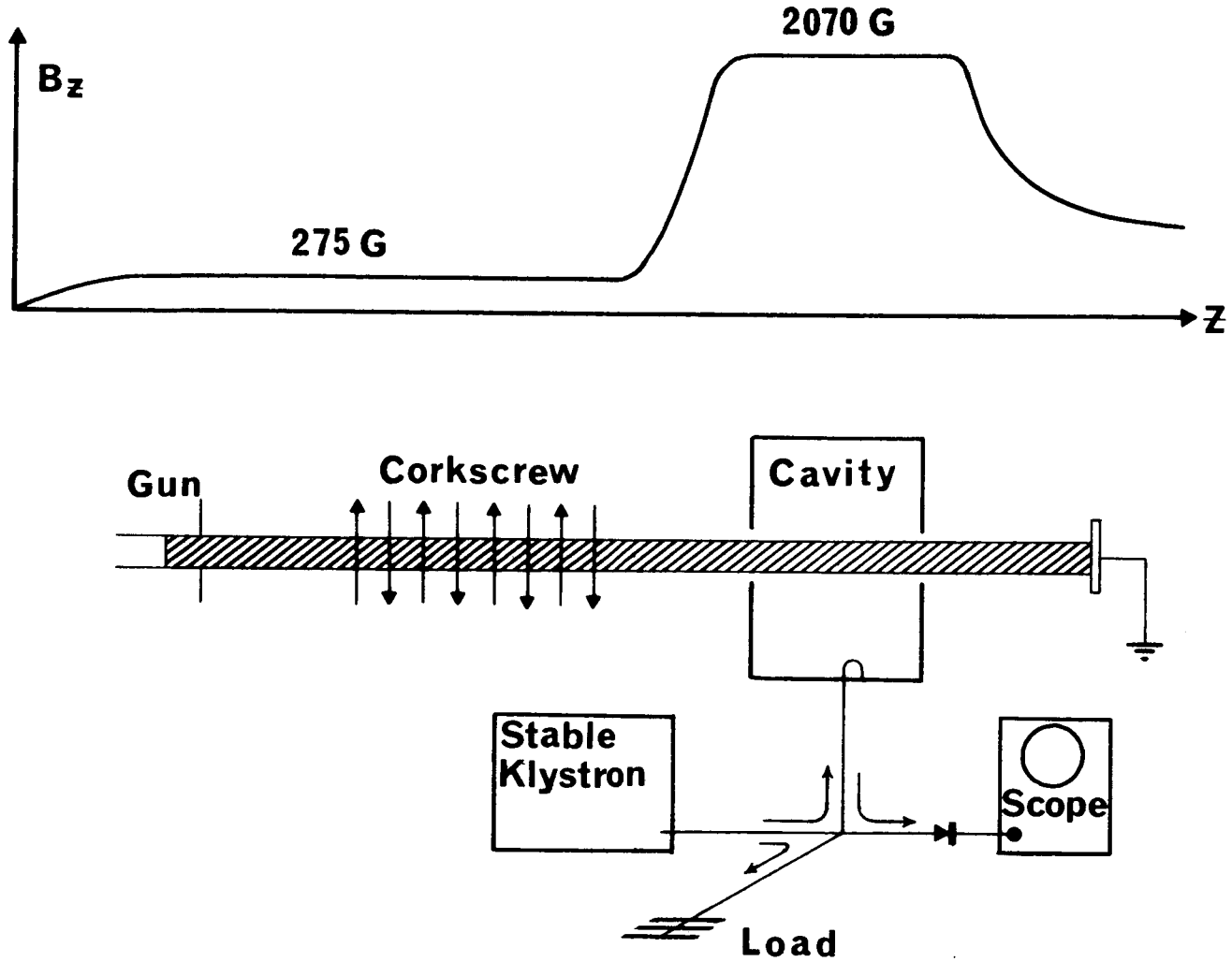

Fig. 5. Illustration of the experimental method. The plot shows the axial magnetic field along the tube.

a 35 cycle/sec rate across cyclotron resonance. Magnetic field increases from right to left. For this photograph the electrons were accelerated through a potential of 5 keV. The absorption line at the higher magnetic field strength which resembles the plane wave prediction for negative absorption by relativistic electrons that suffer collisions according to the relaxational approximation appeared only when the current in the corkscrew magnetic field winding was adjusted to within a narrow critical range.

A purely absorptive resonance always appeared at lower magnetic field strengths than the characteristically relativistic line. It was present for any setting of the current in the corkscrew winding provided that there were high energy electrons in the tube. If the corkscrew were not operating, high energy electrons would spend so short a period of time in the microwave cavity that their cyclotron resonance absorption of cavity field energy would be immeasurably small. The purely absorptive line is therefore attributed to low energy secondary electrons which are emitted when high energy electrons hit the collector. These cold electrons presumably drift along magnetic field lines into the cavity and interact with the cavity fields when the magnetic field strength satisfies the cyclotron resonance condition for non-relativistic electrons.

Further evidence for this interpretation has been obtained by measuring the magnetic field separation between the two resonances. For the data of Fig. 6a the separation of 21 gauss corresponded closely to the expected one percent relativistic

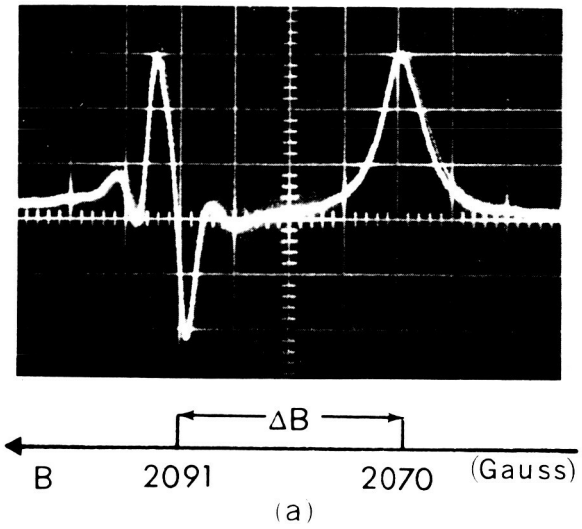

(a)

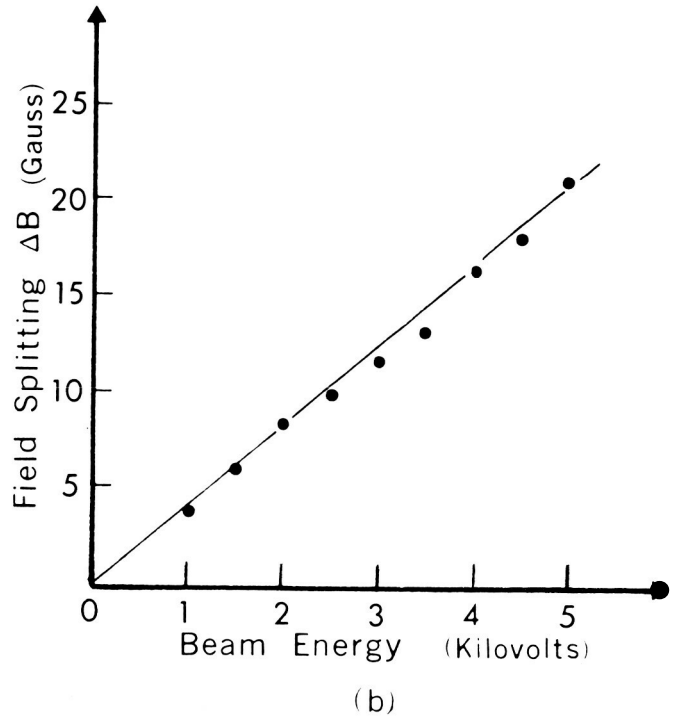

(b)

Fig. 6. (a) Absorption spectrum for 5 keV electrons. (b) Magnetic field separation between the two resonances such as in (a), but as a function of electron energy.

mass increase of 5 keV electrons. This separation has been measured for accelerating potentials below 5 keV and is plotted against the potential in Fig. 6b. Within the accuracy of the measurement the linear relationship agreed with the energy dependence of the mass of weakly relativistic electrons. At accelerating potentials less than 5 keV proper operation of the magnetic corkscrew required a reduction in the 275 gauss axial field in the corkscrew region.

For collector currents in excess of 200 microamperes the negative absorption of field energy by the electrons exceeded the energy lost to the cavity walls and to the coupled coaxial line. The high Q of the cavity ($\sim 10^4$) and small coupling coefficient ($\sim .15$) held these losses to a low enough value to allow the system to support self sustained spontaneous oscillation. The oscillation occurred for magnetic field strengths in the range of the negative portion of the absorption curve observed at low electron densities. The measured output power into the coaxial line was 10 milliwatts.

The collector current necessary to support a self sustained oscillation depended critically upon the effectiveness of the corkscrew magnetic field. If the corkscrew magnetic field was high but not high enough to cut off the beam at the magnetic mirror, little current was needed since the electrons remained in the cavity for longer time intervals. As a general rule, the larger the total electron gun current, the smaller the minimum corkscrew magnetic field strength that was necessary for the system to oscillate spontaneously. This feature is consistent with the

idea that the time interval which the electrons spend in the cavity plays the role of the relaxation time ν_c^{-1} used in the plane wave analysis.

The oscillation spectrum depended significantly upon the total electron gun current and upon the corkscrew magnetic field strength. For low currents and smaller corkscrew magnetic fields the oscillation was localized to within a narrow frequency range. At higher gun currents and lower beam drift velocities the spectrum was broad and markedly structured. In Fig. 7 the spectra for a high value of total gun current and various values of corkscrew magnetic field strength are shown. The measurements were made on a microwave spectrum analyzer. Relative power is measured on the logaithmic scale at the left and the total horizontal frequency sweep is 2 Mc/sec. The accelerating potential for these spectra was 5 keV and the total current drawn from the cathode was 50 milliamperes. The threshold oscillation condition was attained for a corkscrew magnetic field which allowed 28 milliamperes to traverse the magnetic mirror. As the corkscrew field was increased this current (measured at the collector) decreased, the electrons spent a longer average time interval in the cavity and the spectrum broadened. The character of the spectra may depend upon a saturation mechanism which is not well understood.

5. A Theoretical Calculation for the Observed Cyclotron Resonance Interaction

In this section cyclotron resonance absorption by an electron beam which traverses a cavity in a uniform magnetic field is

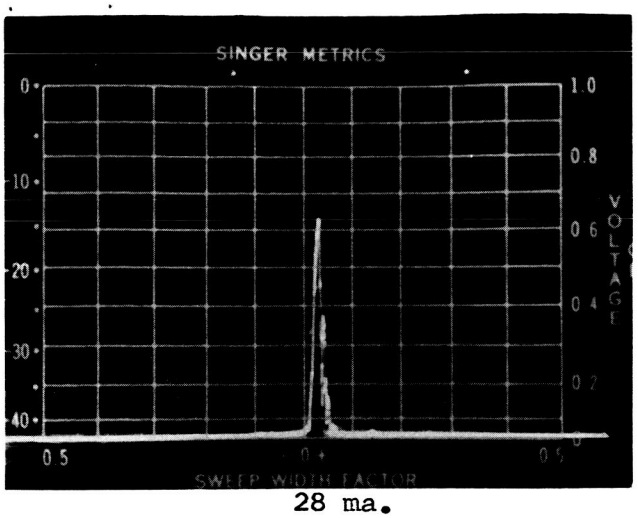

28 ma.

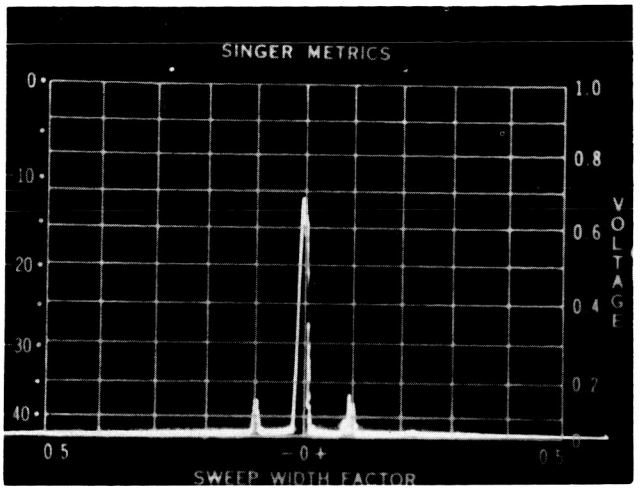

15 ma.

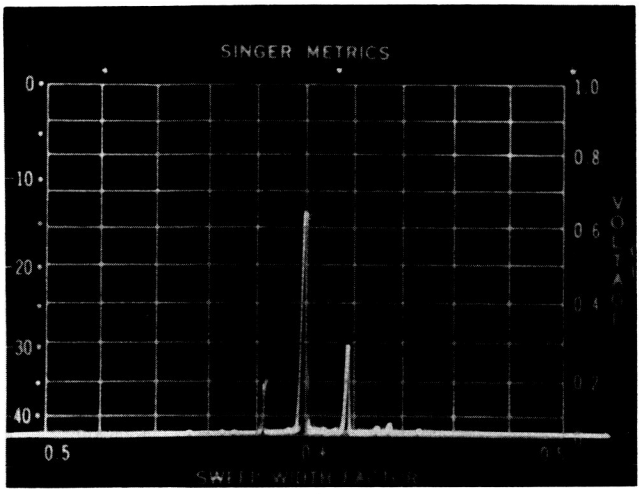

6 ma.

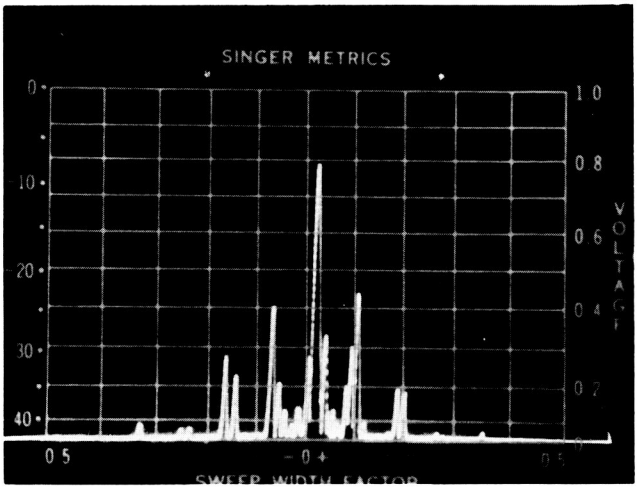

3 ma.

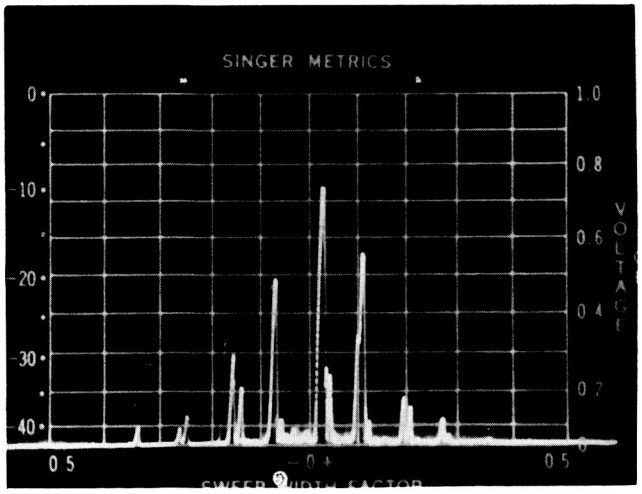

1.5 ma.

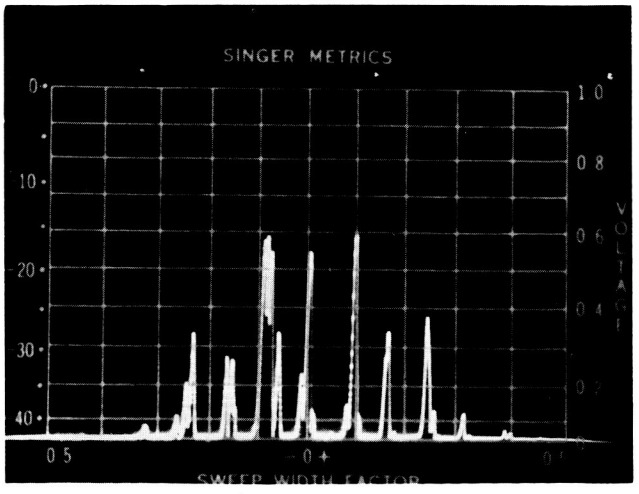

0.8 ma.

Fig. 7. Oscillation spectra for various settings of the corkscrew magnetic field strength. The total cathode current is 50 milliamperes and the current indicated is the collector current. The total frequency sweep is 2 Mc/sec.

analyzed. A theoretical prediction is obtained for the absorption spectrum whose experimental measurement has just been described. In the calculation full advantage is taken of the boundary conditions imposed by the experimental configuration. These boundary conditions are, to summarize, the confinement of the time varying fields to the cavity volume and the fact that for electrons which have not passed through the cavity, the distribution of electron momenta is unperturbed by these fields.

The electrons move along orbits which closely correspond to the helical motion of electrons in a uniform, constant magnetic field because in the perturbation scheme used, the cavity fields $\underline{E}_1$ and $\underline{B}_1$ are assumed to be small. Following a method used by Drummond[24] the linearized Boltzmann equation will be integrated along these unperturbed orbits to arrive at a perturbed distribution function which varies smoothly between the ends of the cavity at z = 0 and at z = L. The electrons are assumed to drift in the positive z direction only hence the perturbed part of the distribution function $f_1(\underline{p},\underline{r},t)$ is zero at z = 0. Moreover, if the electron beam has reached a steady state, $f_1(\underline{p},\underline{r},t)$ will depend upon the displacement r of the beam from the cavity axis only through the dependence of the cavity field amplitude upon r. Its only time dependence will be at the frequency of the cavity fields.

The calculation for f_1 is carried to first order in the amplitude of the cavity oscillation. In an analysis of the perturbation scheme it is shown that the time independent distribution function $f_o(\underline{p},\underline{r})$ may be considered unperturbed by

the cavity fields and thus constant in z to obtain f_1 correct to first order.

A similar perturbation scheme to that used in chapter I is followed here;

$$f = f_o(\underline{p},\underline{r}) + f_1(\underline{p},\underline{r},t) \tag{49}$$

$$\underline{B} = \underline{B}_o + \underline{B}_1(\underline{r},t) \tag{50}$$

$$\underline{E} = \underline{E}_1(r,t) \ . \tag{51}$$

The total distribution function obeys the collisionless Boltzmann equation

$$\frac{\partial f}{\partial t} + \underline{v} \cdot \frac{\partial f}{\partial \underline{r}} + e(\underline{E} + \frac{\underline{v}}{c} \times \underline{B}) \cdot \frac{\partial f}{\partial \underline{p}} = 0 \tag{52}$$

obtained by neglecting the collision term of Eq. (1). Inserting Eqs. (49), (50) and (51) into Eq. (52) one obtains

$$\frac{\partial f_1}{\partial t} + \underline{v} \cdot \frac{\partial f_o}{\partial \underline{r}} + \underline{v} \cdot \frac{\partial f_1}{\partial \underline{r}} + \frac{e}{c} (\underline{v} \times \underline{B}_o) \cdot \frac{\partial f_o}{\partial \underline{p}} + \frac{e}{c} (\underline{v} \times \underline{B}_o) \cdot \frac{\partial f_1}{\partial \underline{p}}$$

$$+ e(\underline{E}_1 + \frac{1}{c} \underline{v} \times \underline{B}_1) \cdot \frac{\partial f_o}{\partial \underline{p}} + e(\underline{E}_1 + \frac{1}{c} \underline{v} \times \underline{B}_1) \cdot \frac{\partial f_1}{\partial \underline{p}} = 0 \tag{53}$$

If this equation is averaged over time, considering the fast periodic time dependence of $\underline{E}_1$, $\underline{B}_1$ and f_1 there results the equation

$$\underline{v} \cdot \frac{\partial f_o}{\partial \underline{r}} + \frac{e}{c} (\underline{v} \times \underline{B}_o) \cdot \frac{\partial f_o}{\partial \underline{p}} + \lim_{T \to \infty} \frac{1}{2T} \int_{-T}^{T} e(\underline{E}_1 + \frac{1}{c} \underline{v} \times \underline{B}_1) \cdot \frac{\partial f_1}{\partial \underline{p}} \, dt$$

$$= 0 \tag{54}$$

Once f_1 is obtained in terms of f_o this last equation may be used to obtain the slow spatial variation of f_o. This would describe the saturation effect which ultimately limits the oscillation level of the device and determines its output spectrum when it is operated as a maser oscillator.

The last term of Eq. (54) is second order in the expansion parameter of the perturbation scheme. The expansion parameter must be proportional to $\underline{E}_1$ and may be chosen as the fractional change of momentum of an electron due to the presence of the small radiation fields $\underline{E}_1$ and $\underline{B}_1$. Thus to first order the last term is neglected and Eq. (54) is satisfied by $f_o(p_\perp, p_\parallel)$ independent of position $\underline{r}$ and independent of the angular momentum space coordinate φ. Consequently f_o may be considered independent of the field amplitude in a calculation for f_1 taken to first order. The calculation proceeds by subtracting Eq. (54) from Eq. (53) leaving rapidly varying first order terms and a second order time averaged term;

$$\frac{\partial f_1}{\partial t} + \underline{v} \cdot \frac{\partial f_1}{\partial \underline{r}} + \frac{e}{c}(\underline{v} \times \underline{B}_o) \cdot \frac{\partial f_1}{\partial \underline{p}} = - e(\underline{E}_1 + \frac{1}{c}\underline{v} \times \underline{B}_1) \cdot \frac{\partial f_o}{\partial \underline{p}}$$

$$- \lim_{T \to \infty} \frac{1}{2T} \int_{-T}^{T} e(\underline{E}_1 + \frac{1}{c}\underline{v} \times \underline{B}_1) \cdot \frac{\partial f_1}{\partial \underline{p}}\, dt \,. \qquad (55)$$

Neglecting the second order term results in an equation for f_1 in which f_o is regarded as a constant function of $p_\perp$ and $p_\parallel$;

$$\frac{\partial f_1}{\partial t} + \underline{v} \cdot \frac{\partial f_1}{\partial \underline{r}} + \frac{e}{c} (\underline{v} \times \underline{B}_o) \cdot \frac{\partial f_1}{\partial \underline{p}}$$

$$= - e(\underline{E}_1 + \frac{1}{c} \underline{v} \times \underline{B}_1) \cdot \frac{\partial f_o}{\partial \underline{p}} \quad . \tag{56}$$

Equation (56) is subjected to some further simplification before inserting the explicit cavity fields for $\underline{E}_1$ and $\underline{B}_1$ and solving for f_1 at all points on the electron beam inside the cavity. It is first noted that the diameter of the electron beam is considerably smaller than the cavity diameter. Secondly, the Larmour radius (radius of the cyclotron orbit) $r_L = p_\perp / |eB_o|$ is yet smaller. For 5 keV electrons in a 2000 gauss magnetic field it is less than 1 mm. The cavity fields are therefore sensibly constant over the diameter of a cyclotron orbit of a single electron. On physical grounds all terms but $v_\parallel \partial f_1/\partial z$ in the second term of the LHS of Eq. (56) are therefore neglected and r, the distance of an electron from the cavity axis, is considered to be a constant in the RHS. This approximation eliminates resonances at harmonics of the cyclotron frequency and greatly simplifies the computations. It is analogous to the neglect of higher order terms in the expansion of the Bessel functions in the plane wave calculation of chapter I. It will be remembered that the argument of the Bessel functions was $k_\perp v_\perp / \Omega = k_\perp r_L$.

For the TE011 mode of a cylindrical cavity the electric field is solenoidal about the cavity axis. The magnetic field of this mode has axial and radial components. To expres Eq. (56)

in a coordinate system (r,θ,z) based upon the cavity symmetry would, however, be awkward. It is easier to take advantage of the fact that the beam is directed parallel to the cavity axis by using a local rectangular coordinate system whose z axis is parallel to the cavity axis and displaced radially from it by a distance r. The geometry of the situation is illustrated in Fig. 8 which shows that the x axis of the local rectangular coordinate system is oriented in the radial direction and that the y axis is parallel to the electric field of the cavity mode. Thus the cavity fields at the electron beam are written

$$\underline{E}_1 = \hat{e}_y \, E_1 J_1(K_\perp r) \sin K_\parallel z \cos \omega t \ , \tag{57a}$$

$$\underline{B}_1 = \hat{e}_x \frac{c}{\omega} K_\parallel E_1 J_1(K_\perp r) \cos K_\parallel z \sin \omega t$$

$$- \hat{e}_z \frac{c}{\omega} K_\perp E_1 J_0(K_\perp r) \sin K_\parallel z \sin \omega t \ , \tag{57b}$$

where $K_\perp = 3.832.../R$ and $K_\parallel = \pi/L$ for a cavity of radius R and length L. Rewriting Eq. (56) in terms of the familiar momentum space coordinates of Eq. (7) and inserting the above expressions for the oscillating fields one obtains

$$\left(\frac{\partial}{\partial t} + v_\parallel \frac{\partial}{\partial z} - \Omega \frac{\partial}{\partial \varphi}\right) f_1 = - eE_1 J_1(K_\perp r)\left[\frac{\partial f_o}{\partial p_\perp} \sin \varphi \sin K_\parallel z \cos \omega t\right.$$

$$\left. + \frac{K_\parallel}{\gamma m \omega}\left(p_\parallel \frac{\partial f_o}{\partial p_\perp} - p_\perp \frac{\partial f_o}{\partial p_\parallel}\right)\sin \varphi \cos K_\parallel z \sin \omega t\right] . \tag{58}$$

Momentum and velocity space coordinates are related by $\underline{p} = \gamma m \underline{v}$ with $\gamma = (1 + p^2/m^2c^2)^{\frac{1}{2}}$. The RHS of Eq. (58) was calculated

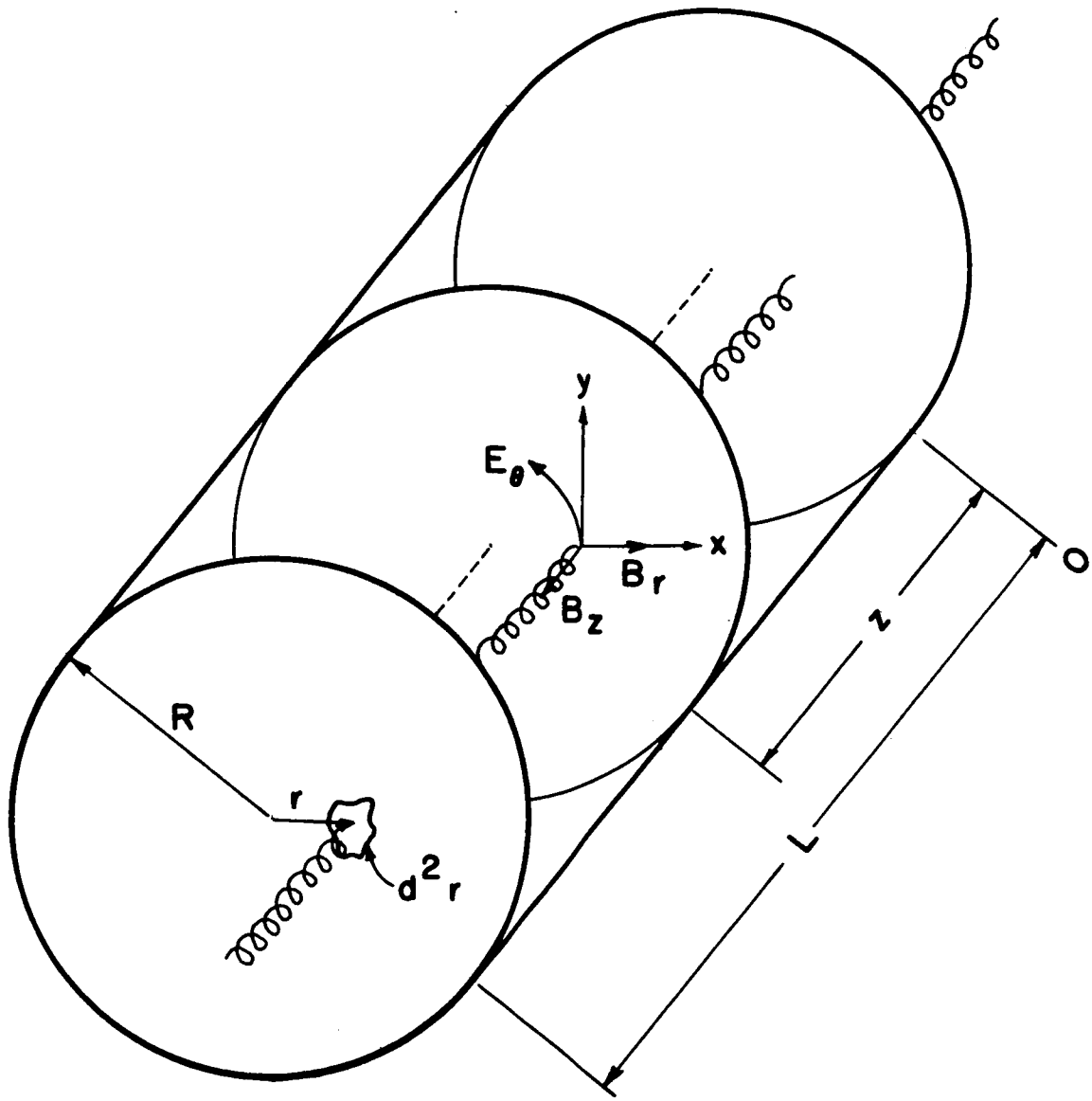

Fig. 8. Coordinate system for the integration of the linearized Boltzmann equation along the unperturbed orbit of an electron.

using the expression $\hat{e}_x(\partial f_o/\partial p_\perp)\cos\varphi + \hat{e}_y(\partial f_o/\partial p_\perp)\sin\varphi + \hat{e}_z\,\partial f_o/\partial p_\parallel$ for the momentum space gradient of f_o independent of φ.

The procedure introduced by Drummond[24] is now used to solve Eq. (58) for f_1. It is essentially the method of characteristics for solving a first order linear partial differential equation. The characteristic curves for the operator on the LHS of Eq. (58) are just the unperturbed orbits in a single particle phase space of an electron in the magnetic field $\underline{B}_o$. The constants of motion of these orbits are distributed according to $f_o(p_\perp, p_\parallel)$. The equations of motion

$$\frac{d\underline{v}'(\tau)}{d\tau} = \frac{e}{c}\,\underline{v}'(\tau) \times \underline{B}_o \tag{59a}$$

$$\frac{d\underline{r}'(\tau)}{d\tau} = \underline{v}'(\tau) \tag{59b}$$

are readily integrated to give

$$z'(\tau) = z + v_\parallel \tau \tag{60a}$$

$$p_\perp'(\tau) = p_\perp \tag{60b}$$

$$\varphi'(\tau) = \varphi - \Omega\tau \tag{60c}$$

$$p_\parallel'(\tau) = p_\parallel \tag{60d}$$

$$t'(\tau) = t + \tau \tag{60e}$$

The constants of integration are chosen so that these primed

variables become the independent variables $(p_\perp, \varphi, p_\parallel, z, t)$ when $\tau = 0$. It is easily verified that

$$\frac{df_1}{d\tau} = \frac{\partial f_1}{\partial t'}\frac{\partial t'}{\partial \tau} + \frac{\partial f_1}{\partial z'}\frac{\partial z'}{\partial \tau} + \frac{\partial f_1}{\partial \varphi'}\frac{\partial \varphi'}{\partial \tau} = \frac{\partial f_1}{\partial t'} + v_\parallel \frac{\partial f_1}{\partial z'} - \Omega \frac{\partial f_1}{\partial \varphi'} . \quad (61)$$

Rewriting Eq. (58) in terms of the primed variables one obtains

$$\frac{df_1}{d\tau} = - eE_1 J_1(K_\perp r)\left[\frac{\partial f_o}{\partial p_\perp} \sin(\varphi-\Omega\tau) \sin K_\parallel(z+v_\parallel\tau) \cos \omega(t+\tau)\right.$$

$$\left. + \frac{K_\parallel}{\gamma m\omega}\left(p_\parallel \frac{\partial f_o}{\partial p_\perp} - p_\perp \frac{\partial f_o}{\partial p_\parallel}\right)\sin(\varphi-\Omega t) \cos K_\parallel(z+v_\parallel t) \sin \omega(t+\tau)\right]. \quad (62)$$

Integrating on τ from $\tau = -z/v_\parallel$ to $\tau = 0$ gives

$$f_1 = - eE_1 J_1(K_\perp r)\left[\frac{\partial f_o}{\partial p_\perp} I_1 + \frac{K_\parallel}{\gamma m\omega}\left(p_\parallel \frac{\partial f_o}{\partial p_\perp} - p_\perp \frac{\partial f_o}{\partial p_\parallel}\right) I_2\right] \quad (63)$$

where

$$I_1 = \int_{-z/v_\parallel}^{o} \sin(\varphi-\Omega\tau) \sin K_\parallel(z+v_\parallel\tau) \cos \omega(t+\tau)d\tau , \quad (64a)$$

$$I_2 = \int_{-z/v_\parallel}^{o} \sin(\varphi-\Omega\tau) \cos K_\parallel(z+v_\parallel\tau) \sin \omega(t+\tau)d\tau . \quad (64b)$$

The limits of integration are due to the constants of motion of Eqs. (60) which require that

$$f_1(p_\perp',\varphi',p_\parallel',z',t') = \begin{cases} f_1(p_\perp,\varphi,p_\parallel,z,t) \text{ for } \tau = 0 \\ 0 \text{ for } \tau = -z/v_\parallel \end{cases} . \qquad (65)$$

The factor $(p_\parallel \partial f_o/\partial p_\perp - p_\perp \partial f_o/\partial p_\parallel)$ in Eq. (63) originates with the magnetic field of the cavity mode. It vanishes for isotropic distribution functions $f_o(p)$ and this explains its absence in the plane wave calculation of chapter I which was carried through with the intent of showing that the growth mechanism persists for isotropic distribution functions. Its effect upon the absorption spectrum to be calculated now will be discussed shortly.

The quantity which has been experimentally measured is the average rate of absorption of cavity field energy by the electrons. The instantaneous rate at which energy is absorbed by an electron of velocity $\underline{v}$ at a point $\underline{r}$ in the cavity is $e\underline{E}_1(\underline{r})\cdot\underline{v}$. The time averaged rate of energy absorption by all electrons in the cavity may thus be formally written

$$\mathbb{P} = \lim_{T\to\infty} \frac{1}{2T} \int_{-T}^{T} dt \int d^3r \int d^3p \; e\underline{E}_1\cdot\underline{v}\; f_1(\underline{p},\underline{r},t)\; n(\underline{r}). \qquad (66)$$

Applied to the configuration of fields considered here this becomes

$$\mathbb{P} = \lim_{T\to\infty} \frac{1}{2T} \int_{-T}^{T} dt$$

$$\int d^2r\; n(r) J_1(K_\perp r) \int_0^L dz\; \sin K_\parallel z \int_0^\infty p_\perp dp_\perp \int_0^{2\pi} d\varphi\; \sin\varphi \int_0^\infty dp_\parallel \frac{e}{\gamma m}\, p_\perp E_1 \cos\omega t\; f_1. \qquad (67)$$

Evaluating the integrals I_1 and I_2 of Eqs. (64a,b), inserting the result in Eq. (63) to obtain f_1 and inserting f_1 in Eq. (67) gives after performing the integrations over φ and z

$$\mathbb{P} = \frac{\pi\rho e^2 E_1^2}{2K_\parallel^2} \int_o^\infty \frac{dp_\parallel}{p_\parallel^2} \int_o^\infty p_\perp^2 dp_\perp \left\{ \frac{\Omega_o}{\gamma\omega} p_\parallel \frac{\partial f_o}{\partial p_\perp} - \left(\frac{\gamma\omega+\Omega_o}{\gamma\omega} \right) p_\perp \frac{\partial f_o}{\partial p_\parallel} \right\} G(x) \quad (68)$$

The following abbreviations are used in Eq. (68):

$$\rho = \int d^2r \; n(r) \; J_1^2(K_\perp r) \; , \quad (69)$$

$$G(x) = \left[\frac{\cos \frac{\pi x}{2}}{1 - x^2} \right]^2 \; , \quad (70)$$

and

$$x = - m \frac{\gamma\omega + \Omega_o}{K_\parallel p_\parallel} \; . \quad (71)$$

After an integration by parts Eq. (68) becomes

$$\mathbb{P} = \frac{\pi\rho e^2 E_1^2}{K_\parallel^2} \int_o^\infty \frac{dp_\parallel}{p_\parallel} \int_o^\infty p_\perp dp_\perp \; f_o(p_\perp, p_\parallel) \; G(x) \left\{ 1 \right.$$

$$\left. + \frac{K_\parallel p_\perp^2}{\gamma m \omega p_\parallel} \left[x\left(1 + \frac{p_\parallel^2}{p_\perp^2} \right) - \frac{1}{2G} \frac{dG}{dx} \left(\frac{\omega^2}{K_\parallel^2 c^2} - x^2 \right) \right] \right\} \quad (72)$$

At this point it is expedient to establish the physical significance of the various terms in Eq. (72). Beginning from the left the quantity ρ defined in Eq. (69) expresses the dependence of the absorption upon the electron density and upon

the amplitude of the cavity oscillation. The density varies only in a plane perpendicular to the cavity axis and in Eq. (69) it is weighted according to the radial variation of the cavity field energy density. The integration extends over the cross sectional area of the electron beam. The function G(x) defined in Eq. (70) is sharply peaked about x = 0. It is the analog of the Lorentzian resonance function of the plane wave analysis. Its precise shape is shown in the plot of Fig. 9. The variable x defined in Eq. (71) is the difference between the frequency of the cavity oscillation and the cyclotron frequency of an electron of momentum $p = (p_\perp^2 + p_\parallel^2)^{\frac{1}{2}}$ measured in units of π times the inverse of the time interval the electron spends in the cavity. This establishes on an analytical basis the equivalence of the roles of the transit time in the present context with the relaxation time ν_c^{-1} in the plane wave analysis.

Of the terms in the curly brackets of Eq. (72) only the quantity 1 survives in the non-relativistic limit because the factor multiplying the other terms (in the square brackets) is of the order of $v_\perp^2/v_\parallel c$. Clearly this is subject to provision that $v_\perp/v_\parallel$ does not tend to infinity. In that case the electrons would remain in the cavity for such long periods of time that the whole linearization procedure would be in doubt since the distribution of electron momenta would be more than slightly perturbed by the cavity fields.

It is instructive to evaluate Eq. (72) for the simple distribution

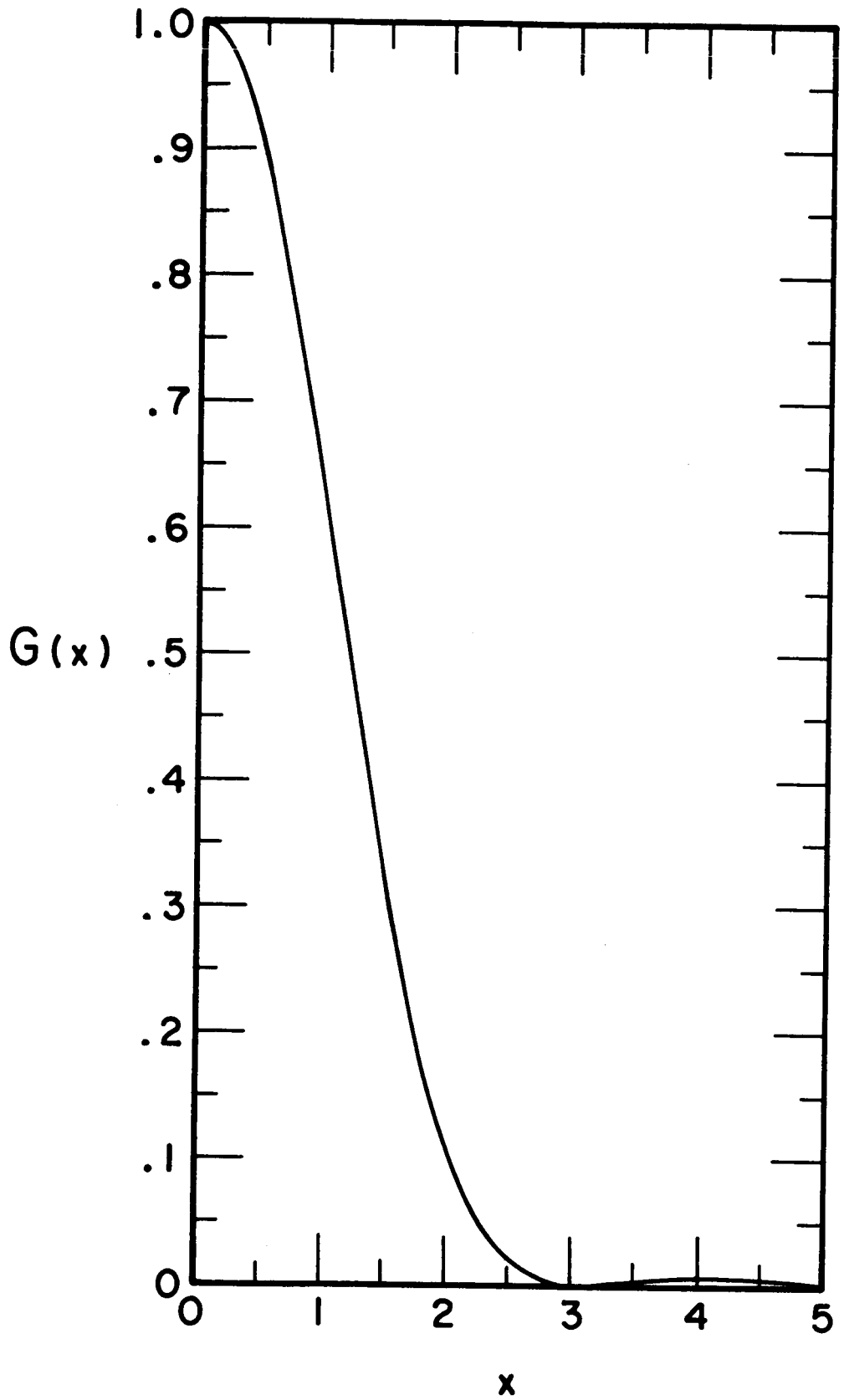

Fig. 9. The resonance function $G(x)=[\cos(\pi x/2)/(1-x^2)]^2$.

$$f_o(p_\perp, p_\parallel) = \frac{1}{2\pi P_\perp} \delta(p_\perp - P_\perp)\, \delta(p_\parallel - P_\parallel) \ . \qquad (73)$$

The absorption spectrum for non-relativistic electrons then has the shape of G(x). The relativistic spectrum for $P_\parallel \ll P_\perp$ follows from Eq. (72) and Eq. (73), neglecting $P_\parallel{}^2/P_\perp{}^2$ relative to unity;

$$\mathbb{P} = \frac{\rho e^2 E_1{}^2}{2K_\parallel{}^2 P_\parallel} \left[\frac{\cos\frac{\pi x}{2}}{1 - x^2}\right]^2 \left\{1 + \frac{\beta}{\lambda}\left[x - \left(\frac{2x}{1-x^2} - \frac{\pi}{2}\tan\frac{\pi x}{2}\right)\left(\lambda^2 - x^2\right)\right]\right\}. \qquad (74)$$

The frequency deviation from exact cyclotron resonance is measured in terms of the variable x evaluated for the specific momenta $P_\perp$ and $P_\parallel$. The absorption spectrum depends upon the two parameters

$$\beta = \frac{P_\perp{}^2}{\gamma m c P_\parallel} = \frac{v_\perp{}^2}{v_\parallel c} \qquad (75)$$

and

$$\lambda = \frac{\omega}{K_\parallel c} \ . \qquad (76)$$

The first represents the effectiveness of the relativistic phase focussing which produces the negative absorption and the second is the length of the cavity in free space half wavelengths. For the TE011 mode $K_\perp{}^2 + K_\parallel{}^2 = \omega^2/c^2$ from which it follows that $\lambda \geq 1$. It is interesting to note that for large values of λ the shape of the absorption spectrum near resonance approaches the result

$$\frac{\rho e^2 E_1^2}{2K_{\parallel}^2 P_{\parallel}} \left[\frac{\cos \frac{\pi x}{L}}{1 - x^2}\right]^2 \left\{1 - \beta\lambda \left[\frac{2x}{1-x^2} - \frac{\pi}{2} \tan \frac{\pi x}{2}\right]\right\}$$

obtained by neglecting the magnetic field of the cavity mode $\underline{B}_1$.

The general result Eq. (74), has been tabulated for a range of values of the parameters λ and β using the facilities of the Yale Computation Center. Near exact cyclotron resonance ($x^2 < 1$) the spectra are substantially similar to the results of the plane wave analysis plotted in Fig. 1. For larger values of $|x|$ the absorption oscillates between positive and negative values. The peripheral oscillations between positive and negative absorption of cavity field energy are, however, severely attenuated by the factor $G(x)$ which diminishes rapidly with increasing $|x|$. The data of Fig. 6 were obtained with a cavity which was approximately three free space half wavelengths long. The computation of Eq. (74) for $\lambda = 3$ and for several values of β is plotted in Fig. 10.

Comparison of the theoretical curve with the measured absorption spectrum shows qualitative agreement in so far as the central portion of the spectrum is concerned. The peripheral wiggles observed experimentally are, however, larger than those theoretically predicted. It is possible that they may be caused by inexact alignment of the cavity axis with the direction of the magnetic field $\underline{B}_0$. The measurements of Fig. 6 were obtained with the electron beam near the cavity axis in which case slight misalignment could cause the beam to cross the axis thus altering the peripheral shape of the spectrum. Data obtained with a

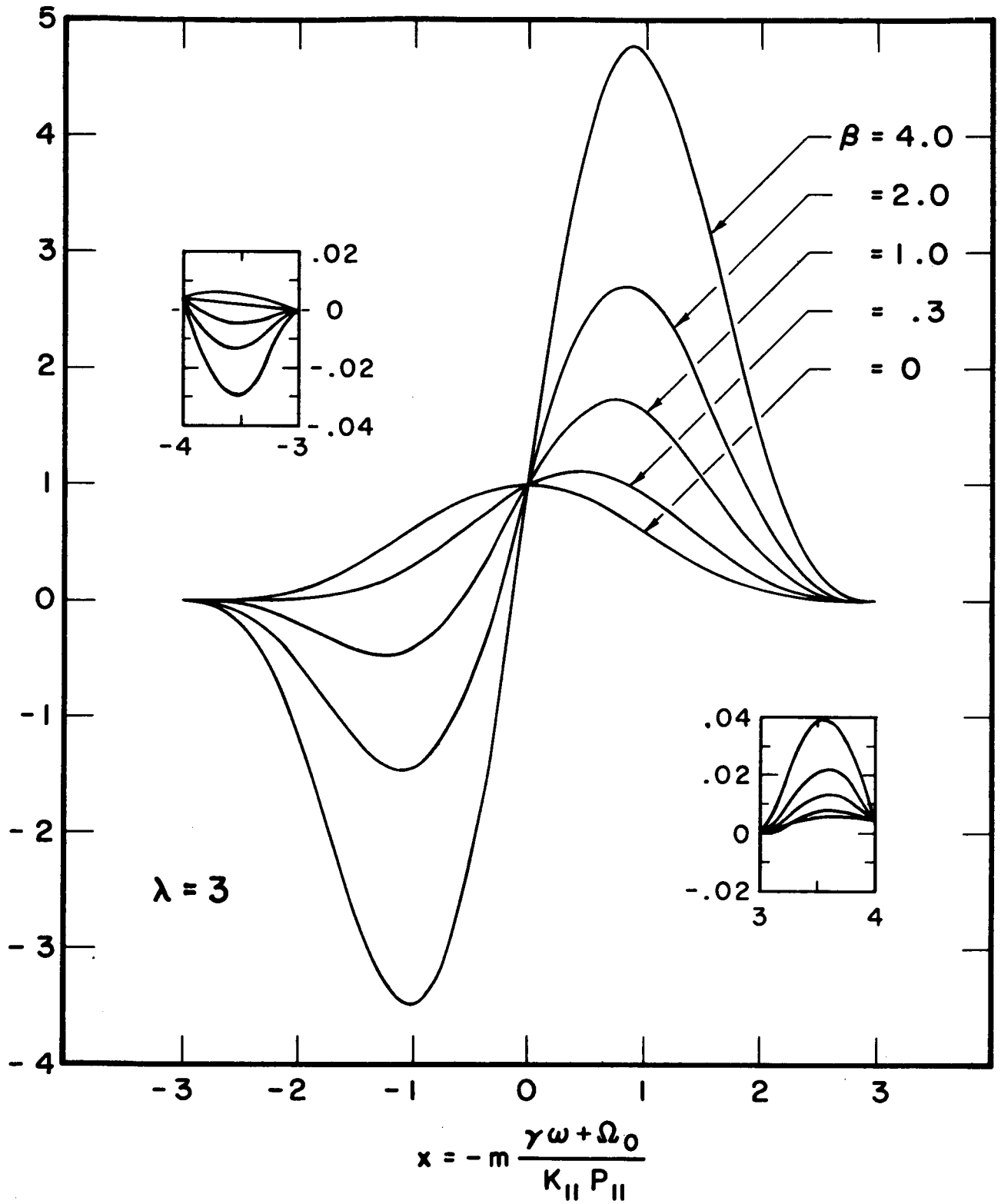

Fig. 10. The shape of the absorption spectrum predicted by Eq. (74) for $\lambda=\omega/K_{\parallel}c=3$ and for various values of $\beta=v_{\parallel}^2/v_{\parallel}c$.

longer cavity ($\lambda \approx 4$) with the beam displaced from the axis exhibited no such wiggles. Indeed, they are theoretically so small that they should not be clearly distinguishable on the oscilloscope display.

The finer details of the absorption spectrum could be obscured by any spread in the distribution of momenta $p_{\parallel}$. These experiments were in fact deficient in this respect since such a spread could easily result from radial inhomogeneities of the corkscrew magnetic field. Within the confines of the experimental configuration no practical method for measuring the actual distribution of parallel momenta was found. Lacking such information no study of the second order effects of the cavity fields upon the time independent distribution function f_o was possible. The validity of the linear analysis was inferred from the constancy of the shape of the absorption spectrum as the cavity field strength was reduced to a level too low to significantly perturb the electron orbits.

III. Pulse Stimulated Cyclotron Radiation from Weakly Relativistic Electrons

1. The Response of Monoenergetic Electrons to a Pulse of Cyclotron Resonance Radiation

An effect is now discussed which is related to the negative cyclotron resonance absorption considered in the last chapter. It will be shown that a system of relativistic electrons such as the kind which will support growing waves near cyclotron resonance responds to a short pulse of radiation at the cyclotron frequency by emitting bursts of coherent radiation some time after the pulse.

The essential features of the effect are described by neglecting the motion of the electrons along the magnetic field, considering them to execute cyclotron motion about fixed centers of rotation in a region of uniform, constant magnetic field. Before the radiation pulse the electrons are monoenergetic. Immediately after it the energy of an individual electron depends upon the phase of its cyclotron rotation with respect to the incident radiation. The effect of the magnetic radiation field is neglected as is the spatial variation of the incident radiation field. Thus a small volume containing many electrons executing cyclotron motion which for a short time experience a circularly polarized radiation field is considered. The electric field lies in a plane perpendicular to the constant magnetic field and rotates in the same sense as the electrons at the cyclotron frequency of the electrons prior to the pulse.

After the pulse the electrons' gyrofrequencies are distributed according to the phase of the electron momentum with respect to the instantaneous direction of electric field during the pulse. Some electrons gain energy from the pulse thus decreasing their gyrofrequencies and others lose energy with consequent decrease in mass and increase of gyrofrequency. The subsequent motion under the influence of the uniform, constant magnetic field alone produces a succession of radiation bursts. It will be shown that the amplitude envelope of these bursts is simply expressed in terms of Bessel functions and is approximately $[J_1(t/\tau)]^2$ for slight perturbation of the initial electron momenta by the exciting pulse.

An important approximation made in the calculation of the radiation emanating from a small volume containing the electrons is that the radiation emitted after the pulse does not affect the electron orbits. Thus the theory is limited to low electron densities where a comparison of the exciting pulse amplitude and maximum radiation amplitude justifies the approximation. The theory predicts that for weak perturbations of the electron orbits, about one third of the total possible coherent emission power into free space will be radiated during the first burst.

The effect bears an interesting relation to negative cyclotron resonance absorption of a steady excitation by virtue of the phase focussing which causes it. The same phase focussing in momentum space that produces the net rotating dipole moment density in response to a pulse also produces currents when the plasma is steadily excited which can feed energy to the wave. There is,

however, one essential difference between the treatment of a steadily excited plasma in the preceding chapters and the kinetic theory of the electron plasma (after experiencing the pulse) to follow. The former involved a perturbation theoretic solution of the Boltzmann equation whereas the latter will involve an exact solution which is a trivial consequence of the Liouville theorem. In the theory the pulse is considered to produce an initial distribution function, the subsequent behavior of which is determined by the incompressible flow of electrons in a single particle phase space demanded by the Liouville theorem.

An experiment which has provided qualitatively corroborating results will be described.

2. A Kinetic Theory Calculation of the Radiation Envelope

In this section a theory is developed which predicts the radiative response of a weakly relativistic ensemble of electrons in a uniform, constant magnetic field to a rotating electric field, applied for a short time duration. The electric field rotates in a plane perpendicular to $\underline{B}_o$. Electron motion parallel to $\underline{B}_o$ is suppressed and the problem is treated in a two dimensional momentum space defined by

$$\underline{p} = \hat{e}_x\, p \cos\varphi + \hat{e}_y\, p \sin\varphi \ . \tag{77}$$

The equation of motion of an electron is written

$$\dot{\underline{p}} = e(\underline{E} + \underline{p} \times \underline{B}_o/\gamma mc) \tag{78}$$

with

$$\gamma = (1 + p^2/m^2c^2)^{\frac{1}{2}} \quad . \tag{79}$$

The electric field is given as

$$\underline{E} = E(\hat{e}_x \sin \omega t + \hat{e}_y \cos \omega t) \tag{80}$$

and is understood not to vanish only for a short time interval Δt.

If Eqs. (77), (79) and (80) are used in the equation of motion Eq. (78) the result

$$\hat{e}_x \frac{d}{dt} (p \cos \varphi) + \hat{e}_y \frac{d}{dt} (p \sin \varphi)$$

$$= \hat{e}_x(\Omega p \sin \varphi + eE \sin \omega t) + \hat{e}_y(-\Omega p \cos \varphi + eE \cos \omega t) \tag{81}$$

is obtained which is equivalent to

$$\frac{d}{dt} (pe^{i\varphi}) = -i\Omega pe^{i\varphi} + ieEe^{-i\omega t} \quad . \tag{82}$$

The usual symbol Ω for the relativistic cyclotron frequency $eB_o/\gamma mc$ is used. The transformation of variables

$$\varphi' = \varphi + \Omega t \tag{83a}$$

$$p' = p \tag{83b}$$

is now introduced. It represents a physical transformation to a momentum space coordinate system (p',φ') rotating with respect to the original system (p,φ) at an angular frequency equal to gyration frequency of the electron's motion in the original

system. It simplifies the solution of Eq. (82) considerably. Rewriting Eq. (82) in terms of the primed variables gives

$$\frac{d}{dt}\left(p'e^{i\varphi'}\right) = ieEe^{-i(\omega-\Omega)t} \tag{84}$$

as the equation of motion of an electron in the rotating momentum space coordinate system.

The frequency ω of the exciting electric field is assumed to be equal to the cyclotron frequency Ω of the electrons before the pulse. In that case the RHS of Eq. (84) is constant for very short time intervals Δt. The implication is that the magnitude and phase of the momentum $\underline{p}$ are changed impulsively and that during Δt the relative phase slip between the momentum $\underline{p}$ and the electric field $\underline{E}$ (due to the change in the cyclotron frequency with changing p) is small. If the maximum change of the cyclotron frequency of an electron from its value Ω at $t = 0$ is $\Delta\Omega$, the condition for negligible phase slip during the pulse may be expressed as $\Delta\Omega\Delta t \ll 1$. For slight perturbations of the momenta of weakly relativistic electrons (i.e. $\Delta p \ll p \ll mc$) the condition is explicitly written

$$\Omega_o \Delta t \ll \frac{m^2c^2}{p\Delta p} \ . \tag{85}$$

The pulse duration Δt is assumed to be small enough to satisfy this inequality and Eq. (84) is integrated trivially from $t = 0$ to $t = \Delta t$ to give

$$p'(\Delta t)e^{i\varphi'(\Delta t)} = p_o'e^{i\varphi_o'} + ieE\Delta t \ . \tag{86}$$

After the pulse ($t > \Delta t$) the RHS of Eq. (84) vanishes and $p'e^{i\varphi'}$ is constant in time. Thus for $t > \Delta t$

$$p'(t)e^{i\varphi'(t)} = p'(\Delta t)e^{i\varphi'(\Delta t)}$$

$$= p_o'e^{i\varphi_o'} + ieE\Delta t \qquad (87)$$

The next step transforms this result for the rotating momentum space coordinates into the result for the non-rotating momentum coordinates by applying Eqs. (83a,b) once more to obtain

$$p(t)e^{i\varphi(t)} = (p_o e^{i\varphi_o} + ieE\Delta t)\, e^{-i\frac{\Omega_o}{\gamma}t} \qquad (88)$$

where

$$\gamma = [1 + (p(t))^2/m^2c^2]^{\frac{1}{2}} \quad .$$

The analysis of the dynamical behavior of a single electron after the pulse is concluded by writing the magnitude of the momentum in terms of its initial momentum coordinates. Multiplying Eq. (88) by its complex conjugative directly gives

$$(p(t))^2 = p_o^2 + 2eE\Delta t p_o \sin\varphi_o + (eE\Delta t)^2 \quad . \qquad (89)$$

An expression for the power radiated by a number N of such electrons confined to a volume larger in dimension than the orbital radius and smaller than the wavelength of the radiation emitted is obtained from Larmor's formula[25] for the total power radiated by an accelerated electron. For an electron in instantaneous circular motion at an angular velocity Ω Larmor's

formula gives

$$\mathbb{P} = \left(\frac{2e^2\Omega_o^2}{3m^2c^3}\right) p^2 \tag{90}$$

In order to calculate the power radiated by N electrons contained in a small volume which have been perturbed by a pulse in the manner described above, p in Eq. (90) is replaced by the statistically summed momentum of the N electrons:

$$\left| \sum \underline{p} \right|^2 = N^2 \left| \int_o^\infty \int_o^{2\pi} p \, dpd\varphi \, f(p,\varphi,t) \, pe^{i\varphi} \right|^2 . \tag{91}$$

The kinetic theory of the problem enters in the integration over momenta distributed according to $f(p,\varphi,t)$ after the pulse.

Since there is no transport of electrons in position space, the incompressible flow of the electron gas in phase space demanded by the Liouville theorem[26,27] requires that

$$f(p(t),\varphi(t),t) \; p \, dpd\varphi = f(p_o,\varphi_o,0) \; p_o dp_o d\varphi_o \tag{92}$$

if $(p(t),\varphi(t))$ are related to (p_o,φ_o) by Eq. (88), the solution of the equation of motion of a single electron. Using this result in Eq. (91) and substituting the RHS of Eq. (88) for $pe^{i\varphi}$ together with Eq. (90) gives for the power radiated as a function of time

$$\mathbb{P} = (\mathbb{P}_o/P_o^2) \left| \int_o^\infty \int_o^{2\pi} p_o^2 dp_o d\varphi_o \, f(p_o,\varphi_o)\left(e^{i\varphi_o} + i\frac{\Delta P}{p_o}\right) e^{-i\frac{\Omega_o}{\gamma}t} \right|^2 \tag{93}$$

where $\mathbb{P}_o = 2N^2e^2\Omega_o{}^2P_o{}^2/3m^2c^3$ is the maximum possible coherent emission rate from N electrons rotating with momentum P_o. In Eq. (93) the abbreviation $\Delta P = eE\Delta t$ is also used and $\gamma = (1 + p_o{}^2/m^2c^2 + 2p\Delta P \sin \varphi_o/m^2c^2 + (\Delta P)^2/m^2c^2)^{\frac{1}{2}}$.

It is reasonable to assume that the electron momenta are distributed uniformly in phase φ_o before the excitation pulse is applied. For convenience the distribution function before the excitation pulse will immediately be taken as the two dimensional isotropic delta function distribution

$$f_o(p_o,\varphi_o) = \frac{1}{2\pi P_o}\,\delta(p_o-P_o) \quad . \tag{94}$$

If the treatment is yet further restricted to weak perturbations of the weakly relativistic momentum P_o such that $\Delta P \ll P_o \ll mc$, Eq. (93) becomes

$$\mathbb{P} = \mathbb{P}_o \left|\frac{1}{2\pi}\int_o^{2\pi} d\varphi_o\,(e^{i\varphi_o} + i\Delta P/P_o)e^{i(\Omega_o t P_o \Delta P/m^2c^2)\sin\varphi_o}\right|^2 \quad . \tag{95}$$

The integration over φ_o is readily performed after expanding the exponential term in a Bessel function series;

$$e^{i(\Omega_o t P_o \Delta P/m^2c^2)\sin\varphi_o} = \sum_{n=-\infty}^{\infty} J_n(\Omega_o t P_o \Delta P/m^2c^2)e^{in\varphi_o} \quad . \tag{96}$$

Only the terms corresponding to $n = 0$ and $n = -1$ survive the integration over φ_o and the final result is

$$\mathbb{P} = \mathbb{P}_o \left[J_1^2(t/\tau) + (\Delta P/P_o)^2 J_o^2(t/\tau)\right] \qquad (97)$$

where

$$\Omega_o \tau = m^2c^2/P_o\Delta P \ .$$

Equation (97) representing the time dependence of the amplitude of pulse excited radiation by N electrons localized in a small volume is a physically useful result only if the rest of space is empty and thus causes no dispersion or absorption of the emitted radiation. In fact Larmor's formula applies only for a single particle in free space and the assumption in the present context is that the ensemble average charge acceleration of closely situated electrons causes the same radiation as a single particle of charge Ne possessing the statistically averaged momentum of the N electrons. If the electrons were spread out over a region comparable in size with the wavelength of cyclotron emission the present model would be inadequate. It would not account for the phase difference of the excitation pulse at various points in the electron gas nor would it account for the interference of the cyclotron radiation emitted by spatially separated groups of electrons. The model offered here is sufficient to illustrate the basic radiative behavior of pulse stimulated relativistic electrons in a uniform magnetic field. It is also a sufficiently comprehensive theoretical model for the experiment to be described as should become evident in the course of its discussion in the section to follow.

The current associated with the first term on the RHS of Eq. (97) vanishes near t = 0 and develops in time as a consequence of the relativistic phase focussing. On the other hand the second term involving J_o is maximum at t = 0. It accounts for the dipole moment induced immediately by the excitation pulse. For $\Delta P \ll P_o$ this term is small and the radiation intensity envelope is closely approximated by the first term alone,

$$\mathbb{P} \approx \mathbb{P}_o \, J_1^2(t/\tau) \; . \tag{98}$$

Experiments have been performed in an effort to observe the time dependence indicated in Eq. (98).

3. The Experimental Method

The apparatus used to verify experimentally the above theoretical considerations is schematically illustrated in Fig. 11. The vacuum system, electron gun, corkscrew magnetic field and axial magnetic field configuration are substantially the same as used in the experiment described earlier although the region immersed in the uniform (±.05 percent) magnetic field $\underline{B}_o$ is longer. The electrons drift consecutively through two microwave cavities in this region. They are separated by a distance L = 35 cm and the electrons interact with their fields over a length ℓ = 3.5 cm.

The corkscrew magnetic field and axial magnetic field in the corkscrew region are carefully adjusted to produce a slowly drifting weakly relativistic electron beam in the cyclotron resonance region. The delta function distribution (given by Eq. (73)) which specifies one particular value of transverse momentum

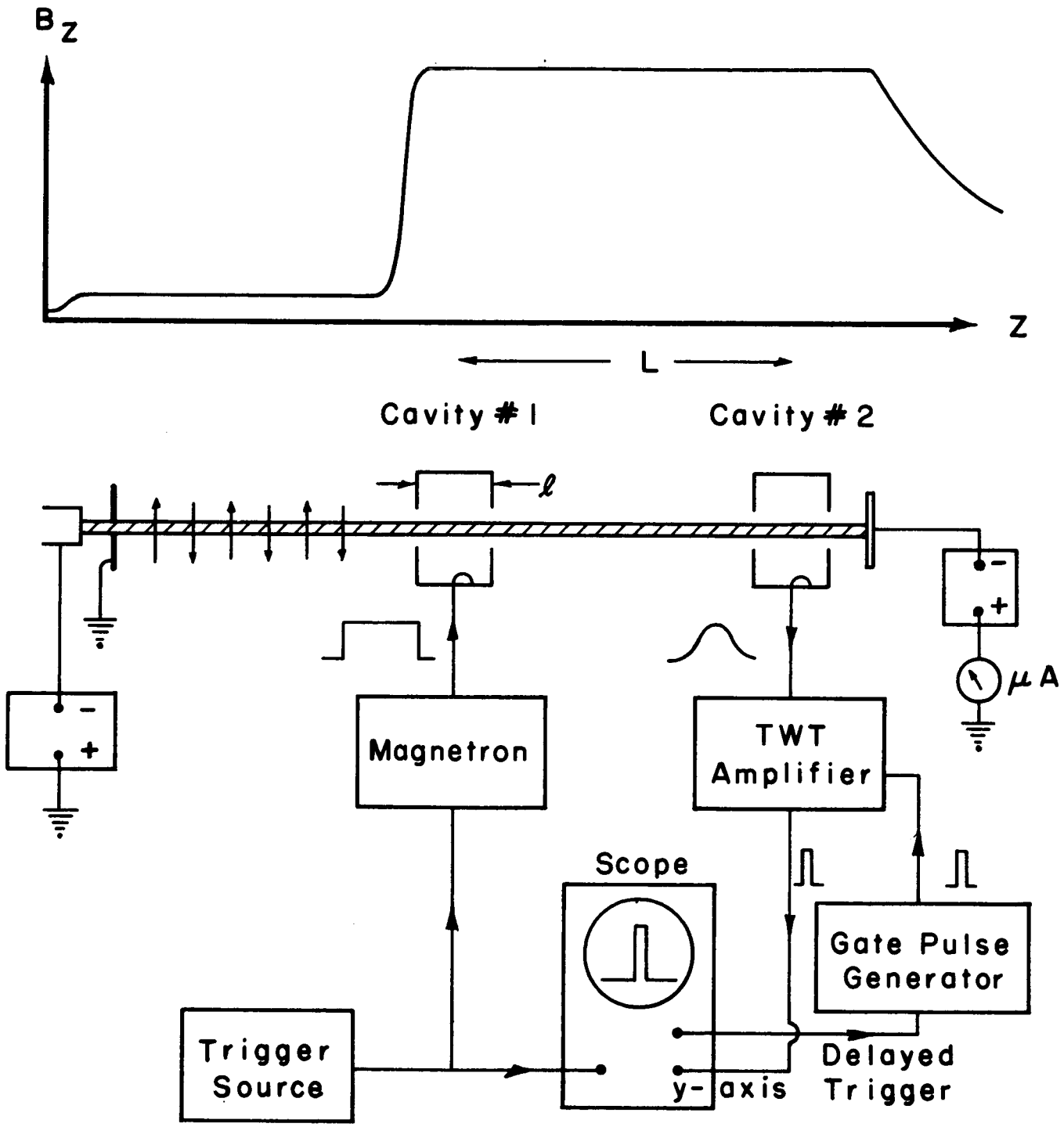

Fig. 11. Illustration of the experimental method for observing pulse stimulated cyclotron radiation. The plot shows the axial magnetic field along the tube.

$P_\perp$ and one value of parallel momentum $P_\parallel$ together with the condition $P_\parallel \ll P_\perp \ll mc$ are considered to describe the beam in that region. As the electrons drift through the first cavity which is driven by an external microwave signal generator, they experimence the excitation pulse for a time interval $\gamma m\ell/P_\parallel$. This time interval is to be associated with Δt of the preceding section. After a delay time $\gamma mL/P_\parallel$ (equal to the time of flight of an electron between the two cavities) the electrons enter the second cavity which functions as a sensitive receiving antenna for the radiation emitted by the electrons within it. This delay time is equivalent to t in Eq. (97) or Eq. (98). Thus for a given setting of the electron beam characteristics the quantities t and Δt are fixed. The natural experimental parameter to vary is the amplitude of the excitation field in the first cavity thereby varying ΔP. The amplitude of the oscillation stimulated in the second cavity by the electrons should therefore reflect the ΔP dependence of the radiation power specified by Eq. (97).

The cavities were designed to resonate in the TM010 mode at 6525 Mc/sec and were oriented so that their axes of cylindrical symmetry were perpendicular to $\underline{B}_o$. Thus the electric field of the mode was perpendicular to $\underline{B}_o$ and the electron beam traversed the cavity diametrically. The cavities were of identical construction, although, for precise alignment, they were made tunable by inserting a tuning slug through one flat end of each. The slug, 1/4 inch in diameter, could penetrate the cavity to a depth of about 3/8 inch along its axis providing a tuning range of 100 Mc/sec. The vacuum integrity of the mechanism was maintained with a stainless steel flexible bellows.

Coupling to the cavities was accomplished through ceramic vacuum windows mounted exactly as for the steady state absorption experiment described earlier. The cavities were joined to sections of 1/2 inch I.D. stainless steel pipe which connected to the magnetic corkscrew section via vacuum flanges. The same water cooled collector as described earlier was used. The entire assembly was fabricated of type 304 non-magnetic stainless steel and all joints were brazed with copper in vacuum or welded in an inert gas atmosphere. After extended bakeout of the entire vacuum chamber operating pressures of 2×10^{-9} mm Hg were achieved.

The microwave electronics consisted basically of a signal generator whose output power could be continuously varied by an attenuator, and a sensitive microwave receiver. The attenuated output of the microwave signal generator was fed to the first cavity and the receiver which consisted of a TWT amplifier and a crystal detector was coupled to the second cavity. The minimum detectable signal for this simple arrangement was 10^{-10} watts.

Referring to Fig. 11 it is observed that the signal source used for the excitation field in cavity No. 1 was a pulsed magnetron and that the receiver was gated. This was done for technical reasons to be described forthwith. It is to be emphasized that the excitation pulse duration is determined only by the time of flight of an electron across cavity No. 1 and that the delay between the excitation pulse and the observation of the resulting cyclotron emission is due only to the time of flight of an electron between the cavities. The intermittently operated

magnetron was used because it was the only available source which provided the required power level.

The receiver was gated in synchronism with the intermittent operation of the magnetron by applying a short rectangular pulse to the grid of the traveling wave tube. The oscilloscope thus measured the rectified output of the TWT amplifier at the same time during each successive magnetron output pulse. The operation of the apparatus therefore simulated steady state operation. The only difference was that instead of measuring the continuous output of microwave energy from cavity No. 2, it was measured over a short period of time.

The magnetron pulse was approximately 400 nanoseconds long. Since the fields in the cavities, for which the Q was about 1600, do not build up too quickly on this time scale the gating of the receiver was crucial. The gate width could be varied between 10 and 100 nanoseconds. The odd shape of the magnetron pulse amplitude envelope also suggested that care be taken to observe the radiation level at the same time in each repetition of the experiment. The recourse to gating the receiver dealt effectively with these problems and there were no ambiguities introduced by using an intermittently operated signal source. It should be added that the repetition rato of the magnetron which operated at 6525 Mc/sec was 700 pulses/sec.

The experiments were performed with low current electron beams ($\sim$ 10 microamperes) so that the TM010 mode oscillation stimulated in the second cavity by the electrons was negligible in amplitude compared with the externally driven oscillation in

the first cavity. This assured that after experiencing the excitation pulse the electrons streamed freely in phase space under the influence of $\underline{B}_o$ alone. Electrostatic effects due to the nonvanishing charge density in the beam were thereby minimized as well.

4. The Experimental Observations

A small retarding potential applied to the collector offered an approximate measure of the electron drift energy in the cyclotron resonance magnetic field region. Optimum values of the transverse and axial corkscrew fields were determined by minimizing the retarding potential necessary to repel the beam. A minimum retarding potential of 10 eV could be achieved. After making these adjustments as well as setting the cyclotron resonance field to exact cyclotron resonance for the particular beam energy used, the excitation to the first cavity was increased from zero. Point by point measurements of the relative amplitude of the oscillation induced in the second cavity as a function of the field amplitude in the first cavity were thereupon made.

The data obtained with a 1.4 keV, 10 microampere electron beam are presented in Fig. 12a. The horizontal scale is proportional to the amplitude of the excitation pulse experienced by an electron as it passed through the first cavity. The amplitude of the oscillation induced in the second cavity is observed to have the expected decaying periodic dependence on the excitation pulse amplitude. For reference purposes the theoretical prediction of Eq. (98) is plotted in Fig. 12b on a scale which

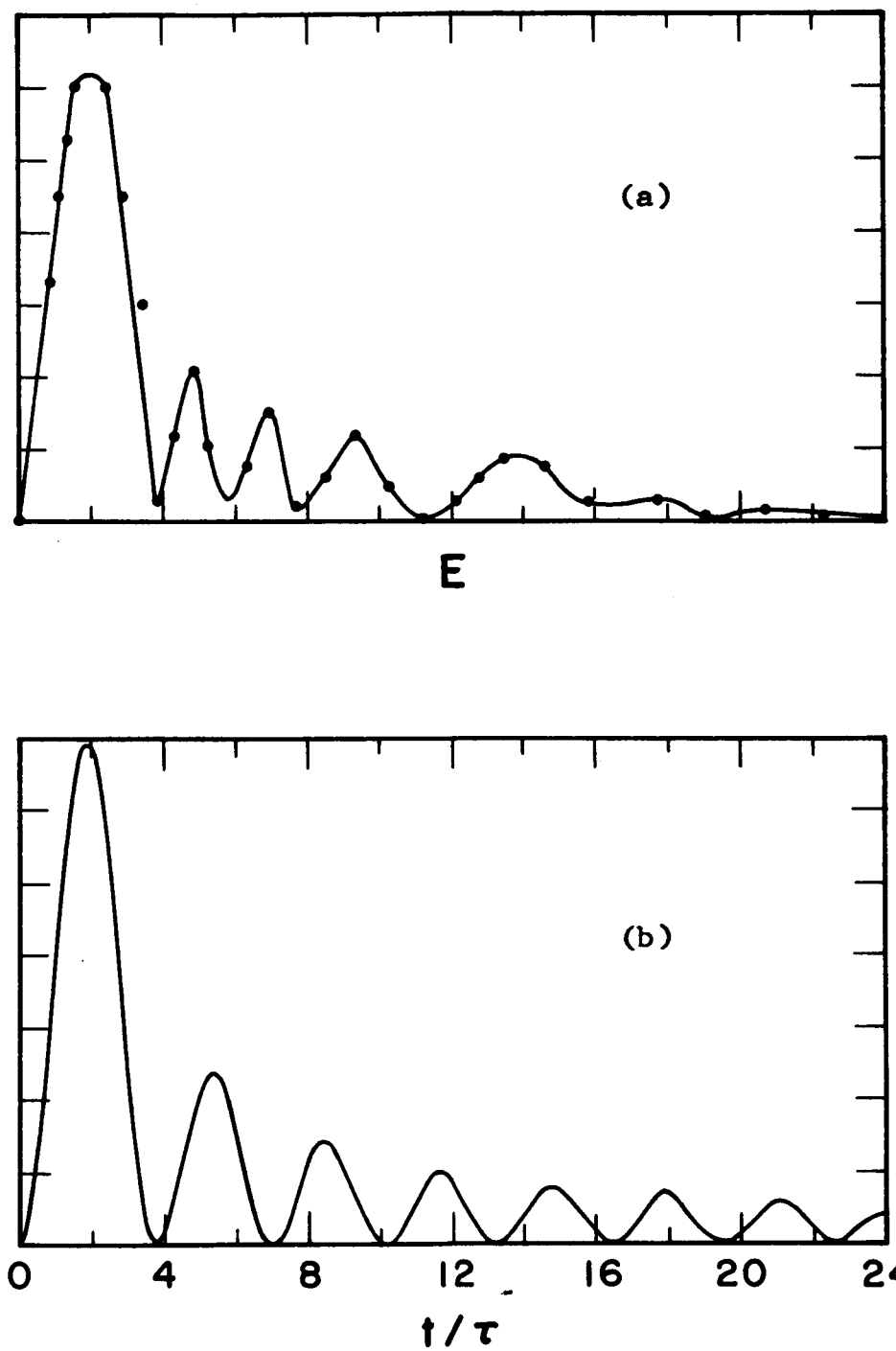

Fig. 12. (a) The measured radiation intensity for 1.4 keV electrons as a function of E, the excitation field strength. E is approximately 4 V/cm at the first peak. (b) The theoretical prediction, $P \sim J_1^2(t/\tau)$.

allows the first experimental peak and the first theoretical peak to coincide.

An approximate value for the excitation field intensity at the first peak was obtained from measurements of the Q, coupling factor and power incident upon the first cavity. For the data of Fig. 12a this electric field was 16 V/cm at the center of the cavity. In view of the fact that the impulse $\Delta P = eE\Delta t$ received by an electron is effectively determined by the average field across the diameter of the cavity this figure should be reduced accordingly. Multiplication by 1/2 gives a reasonable estimate for the average field. A final correction factor, exactly equal to 1/2, enters as a consequence of the linear polarization of the electric field of the cavity mode. The electronic motion is coupled strongly only to that circularly polarized component which rotates in the same sense as the electrons. The effective excitation pulse amplitude E is therefore 4 V/cm. With $\Delta t = \gamma m\ell/P_{\parallel}$, $t = \gamma mL/P_{\parallel}$ and $t/\tau = 1.84...$ the energy of electron drift along $\underline{B}_o$ is calculated to be 20 eV.

No completely satisfactory explanation for the discrepancy between the experimentally measured and theoretically predicted spacing between the peaks is at hand. However, one could not expect the simple result Eq. (98) plotted in Fig. 12b to apply exactly for several reasons. The foremost objection is that the condition for the impulsive approximation used in the electron dynamics is not too strictly adhered to. This condition, expressed in Eq. (85), is equivalent to $\Delta t \ll \tau$. The ratio of the cavity diameter to the inter-cavity distance specifies that

$\Delta t/t = \ell/L = 1/10$. For successive radiation peaks to occur at the second cavity $t/\tau = 1.84, 5.33, 8.53, \ldots$ etc. and the condition is clearly violated for peaks after the third. The fact that the peaks tend to disappear for $\Delta t \sim \tau$ is consistent with this picture.

It is concluded that the effect has been observed, albeit, only to a qualitative degree of accuracy.

IV. Cyclotron Resonance Absorption by Low Energy Electrons Elastically Scattered in a Neutral Gas Background

1. General Remarks

With a shift in emphasis from relativistic phenomena to low energy collision phenomena, negative cyclotron resonance absorption due to electron-neutral atom elastic scattering is now discussed. Ordinarily collisions are regarded as a dissipative mechanism which causes damping of any mode of oscillation in a plasma by destroying the phase order of the motion of the plasma particles. In reality collisions can cause the growth of an oscillation in a non-Maxwellian plasma.[2] This was shown for the case of the cyclotron resonance interaction in a tenuous, monoenergetic, infinite plasma of electrons in chapter I.

The analysis of chapter I assumed that collisions are adequately described by the simple relaxation approximation[14] given in Eq. (8). It would be beyond the intended scope of this work to delve into the theoretical justification for this model as it applies to collisions between electrons and neutral atoms although a few words in support of its use will be said. Its foremost virtue is that it makes the analysis involved in the solution of the linearized Boltzmann equation tractable. Secondly, it has the desired effect of disordering the phase ordered motion associated with first order currents in the perturbation theory used. The ability of the neutral atom scatterers to randomize the first order currents associated with electrons of different energy at different rates is inserted into the model by allowing the collision

frequency ν_c to be functionally dependent upon the magnitude of the momentum of the scattered electron. The electrons are assumed to be scattered elastically.

The relaxation approximation is objectionable on the grounds that it usually does not conserve particle number, momentum and energy which are conserved in elastic collisions. A physically consistent treatment of binary collisions must begin with the Boltzmann collision integral. A connection between the Boltzmann collision integral and the relaxation approximation has been worked out by Desloge and Matthysse.[28] They point out that the appropriate relaxation frequency ν_c is the collision frequency for momentum transfer.

The attitude to be chosen here will be to accept the results of chapter I as suggestive of the existence of negative absorption by slow electrons due to collisions (physical inconsistencies notwithstanding) and to offer a comparison with experimental data. The same technique of microwave spectroscopy as was used in the study of cyclotron resonance absorption by relativistic electrons was used in the presently discussed study of the absorption by slow electrons in a low pressure neutral gas background. The generation of the necessary distribution of electron momenta was not as involved as it was in that work since nothing as complicated as the corkscrew magnetic field device was necessary.

A beam of low energy electrons formed in a region of low magnetic drifted along converging field lines into the uniform cyclotron resonance magnetic field region. The magnetic mirror effect and collisions with neutral gas atoms along the drift path

provided a distribution of momenta between the direction perpendicular to the magnetic field and the direction parallel to it. Thus with a significant part of the energy of the monoenergetic distribution of momenta associated with rotational motion, low field intensity in the microwave cavity and with sensitive detection the validity of the perturbation theory was assured.

The obvious choice of background gases were the rare gases Argon, Krypton and Xenon whose elastic collision cross sections possess a Ramsauer minimum[15] near 1 eV. The cross sections of these gases rise steeply for a few eV above the Ramsauer minimum. A multitude of papers have appeared in the last few years describing the radio frequency and microwave emission and absorption characteristics of discharge tube plasmas of these gases. For the particular case of the cyclotron resonance interaction, among the most notable are the calculations offered by Tanaka and Mitani[29] which extend the earlier work of Bekefi, Hirshfield and Brown[2] and of Twiss.[1] Shortly thereafter Terumichi et al.[30] reported the observation of an anomalously large transmission of radiation at cyclotron resonance through a Xenon discharge plasma and attributed it to the collisional growth mechanism. In a later paper[13] the same authors reported the amplification of a signal incident upon a microwave cavity containing a Xenon discharge in a cyclotron resonance magnetic field. The experiments reported in these papers are singularly deficient in their ability to support the theoretical work since the data is difficult to interpret in anything but a qualitative

sense. One exception to this trend in the experimental work are the measurements of the radiation temperature of various rare gas discharges by Fields, Bekefi and Brown.[31]

In all the experimental work to date the basic shape of the absorption spectrum which exhibits the negative dip illustrated in Fig. 2 could not be resolved because a broad distribution of electron energies was involved. The experiments with monoenergetic distributions (to be described below) were performed in an effort to observe the dip and show that it occurs only for energies at which the cross section for collisions with neutral gas atoms increases sharply with electron energy. Only the phenomena associated with increasing collision frequencies was studied. The predictions of Fig. 3 for decreasing ν_c do not apply to the experiments that were performed.

2. Measurements of the Absorption Spectrum

The apparatus was similar, with a few modifications, to the equipment illustrated in Fig. 4. The configuration of magnetic fields was exactly the same as for the energetic electron absorption experiment with the exception of the corkscrew winding which was eliminated. The microwave cavity, which was smaller, operated in the TM010 mode at 5782 Mc/sec and was oriented with its axis of cylindrical symmetry (and thus its electric field) perpendicular to $\underline{B}_o$. The electron beam traversed the cavity diametrically.

Immediately before entering the cavity the electron beam passed through a grid structure consisting of three parallel

grids in planes perpendicular to the axis of the tube. The grids were approximately 3/16 inch apart and the outer two were electrically grounded to the tube wall. The inner grid was supported by a tungsten wire which passed through the side wall of the tube via a 1/4 inch diameter glass to stainless steel housekeeper seal. A negative square wave potential applied to this grid was used to modulate the electron beam in the cavity. A variable retarding potential applied to a similar grid structure just after the cavity was used to measure the distribution of energy associated with motion along $\underline{B}_o$.

The grid was formed of a commercially available knitted tungsten wire mesh. The 1/16 inch spacing between the .001 inch tungsten wire provided a grid which would transmit 97 percent of the incident electron current. The mesh was sandwiched between circular stainless steel frames which were spot welded together. The frames were then mounted within the tube structure. Assembly of the cavity and grid structures was facilitated by dividing this part of the tube into separate sections machined from stainless steel stock. The completed sections were joined to form a vacuum tight chamber by welding in an inert gas atmosphere. Type 304 non-magnetic stainless steel was used throughout.

The schematic diagram of the apparatus in Fig. 13 shows the microwave spectrometer and detection system which consisted of a TWT amplifier, crystal detector and a lock-in amplifier for synchronous detection of the absorption signal. The reference signal for the synchronous detector was derived from the 10 Kc/sec

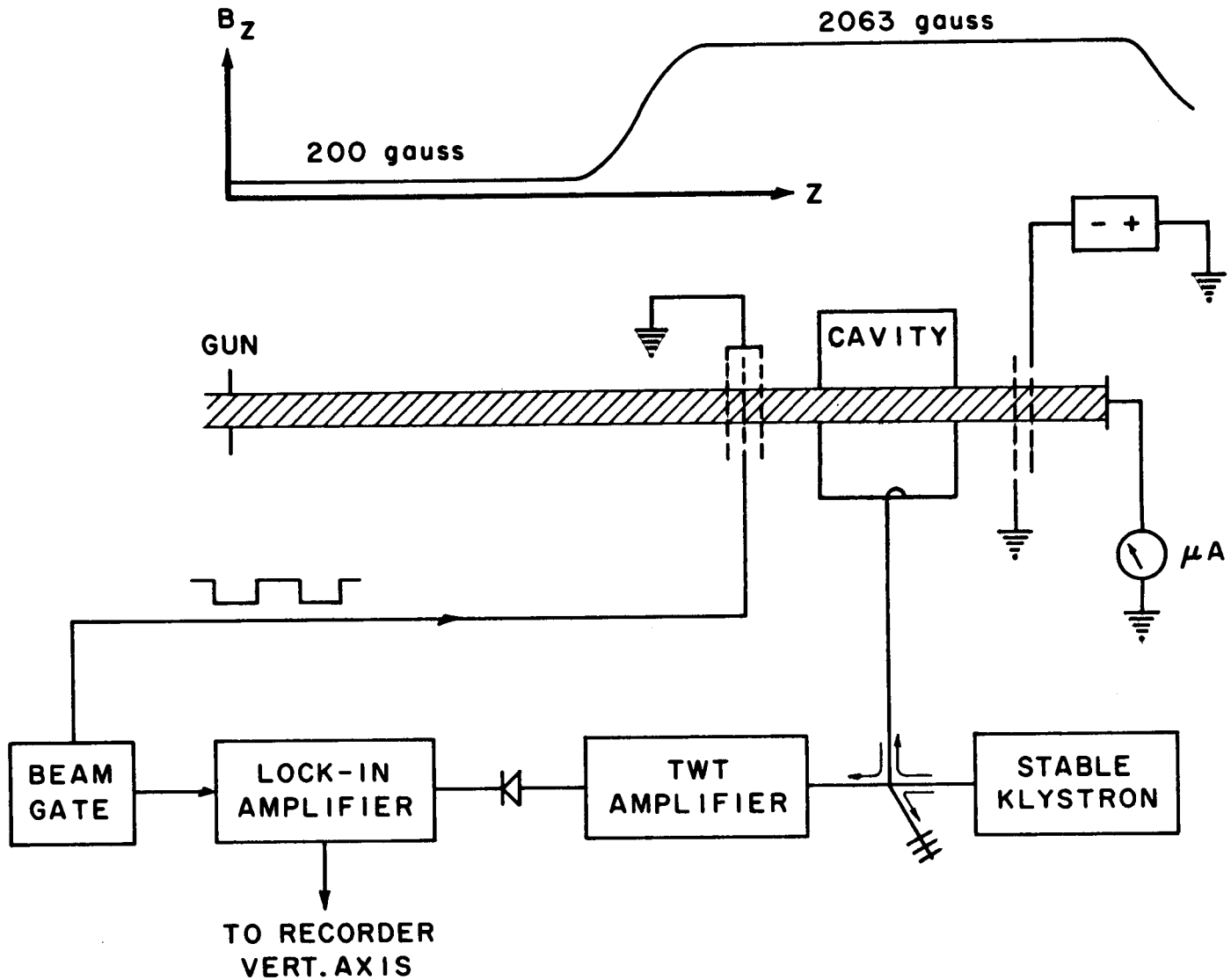

Fig. 13. Illustration of the experimental method for measuring the cyclotron resonance absorption spectrum of slow electrons in a neutral gas background. The plot shows the axial magnetic field along the tube.

negative square wave voltage applied to the beam gating grid. The output of the lock-in amplifier was plotted on the vertical scale of an X-Y recorder whose horizontal trace was swept slowly in synchronism with the cyclotron resonance magnetic field intensity B_o.

The absorption was measured as a function of B_o for various electron gun potentials in vacuum and in the background gases Argon, Krypton and Helium. It was found that the best method for maintaining a constant low background gas pressure (usually less than 10^{-3} mm Hg) was to feed gas to the system via a small aperture leak valve while continuously pumping the system. The data thus obtained is exhibited in Figs. 14 through 17 for Argon, in Figs. 18 through 21 for Krypton and in Figs. 22 and 23 for Helium. The numbers to the upper left of each trace denote the gas pressure measured directly on a Bayard Alpert type ionization gauge which was calibrated for nitrogen. To correct for the difference of the ionization probabilities of the gases used the indicated readings should be multiplied by the following factors:

Argon: multiply by 0.85

Krypton: multiply by 0.53

Helium: multiply by 6.22

These correction factors are quoted from the manufacturer's recommendations.

The narrow absorption line on the right hand side of the spectra is interpreted as the electron cyclotron resonance absorption. Its observed linewidth for electrons in vacuum

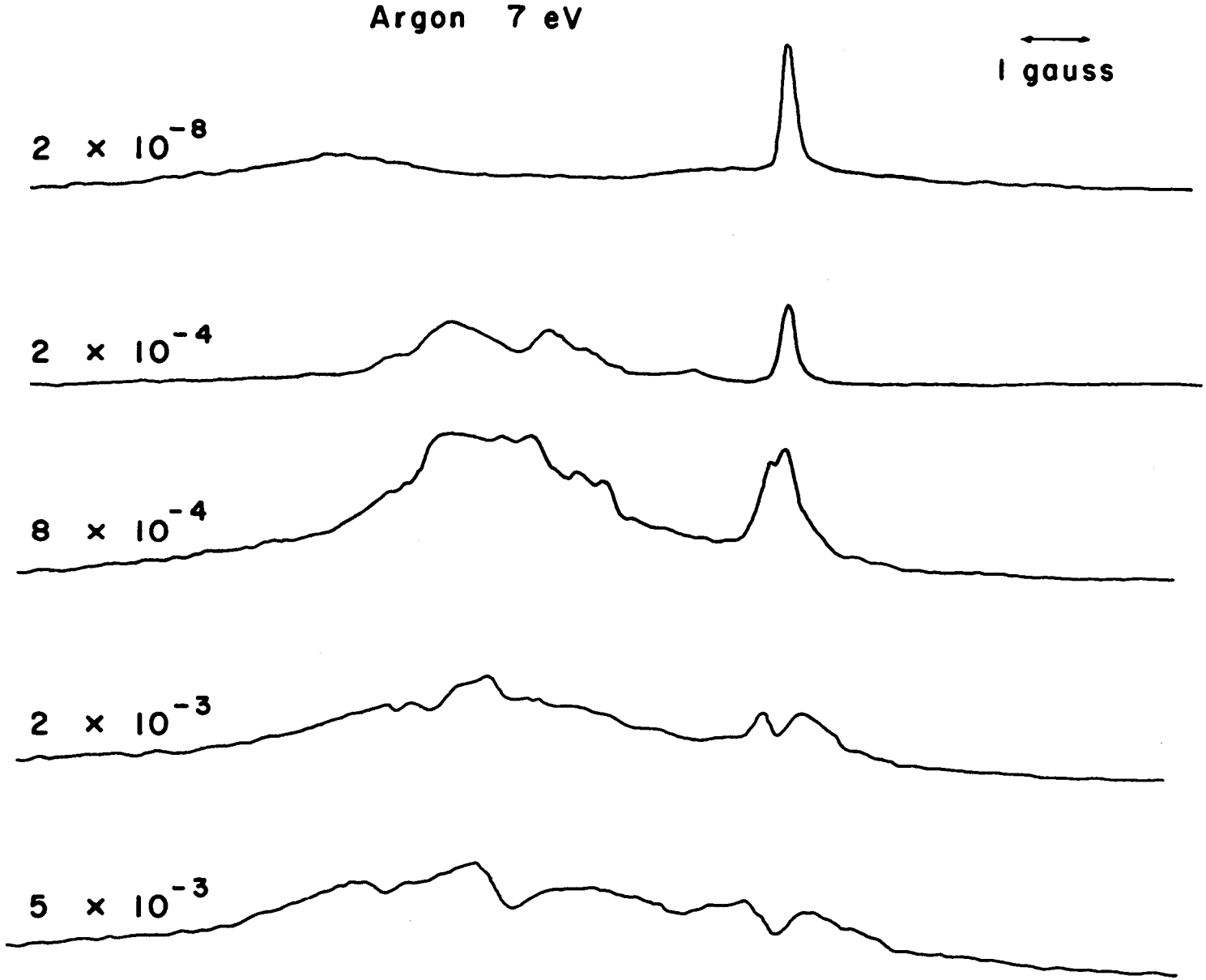

Fig. 14. Cyclotron resonance absorption spectra for 7 eV electrons in Argon.

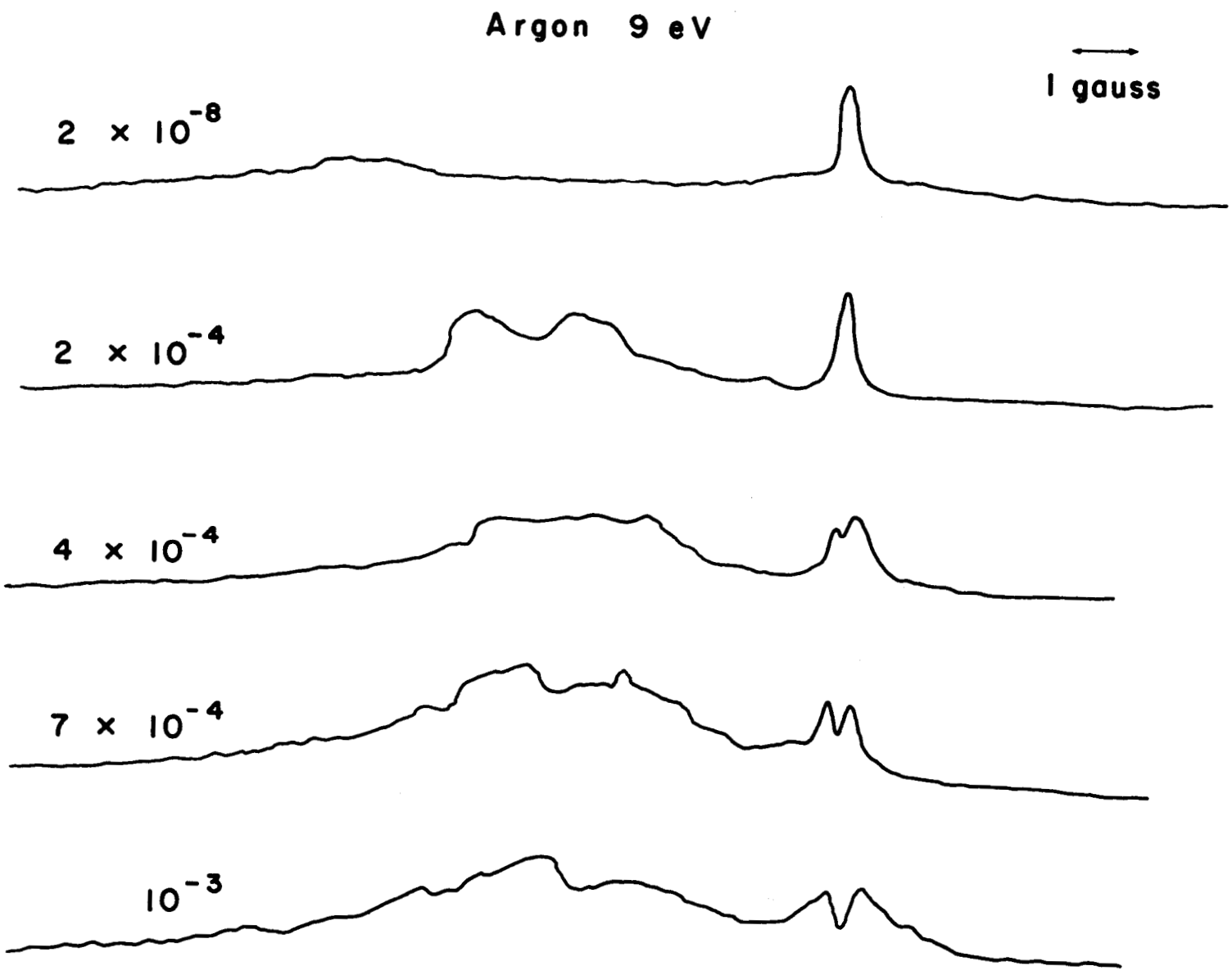

Fig. 15. Cyclotron resonance absorption spectra for 9 eV electrons in Argon.

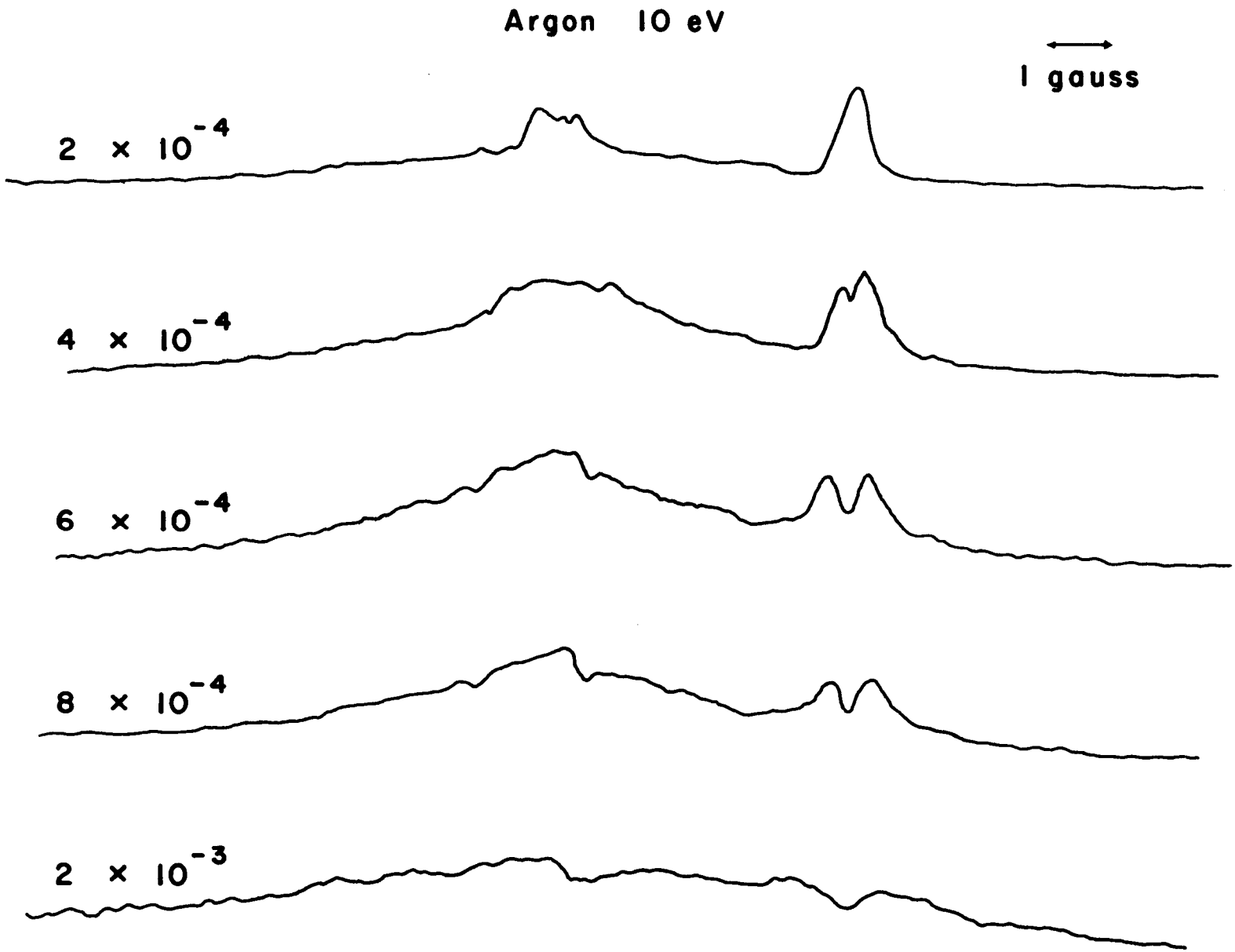

Fig. 16. Cyclotron resonance absorption spectra for 10 eV electrons in Argon.

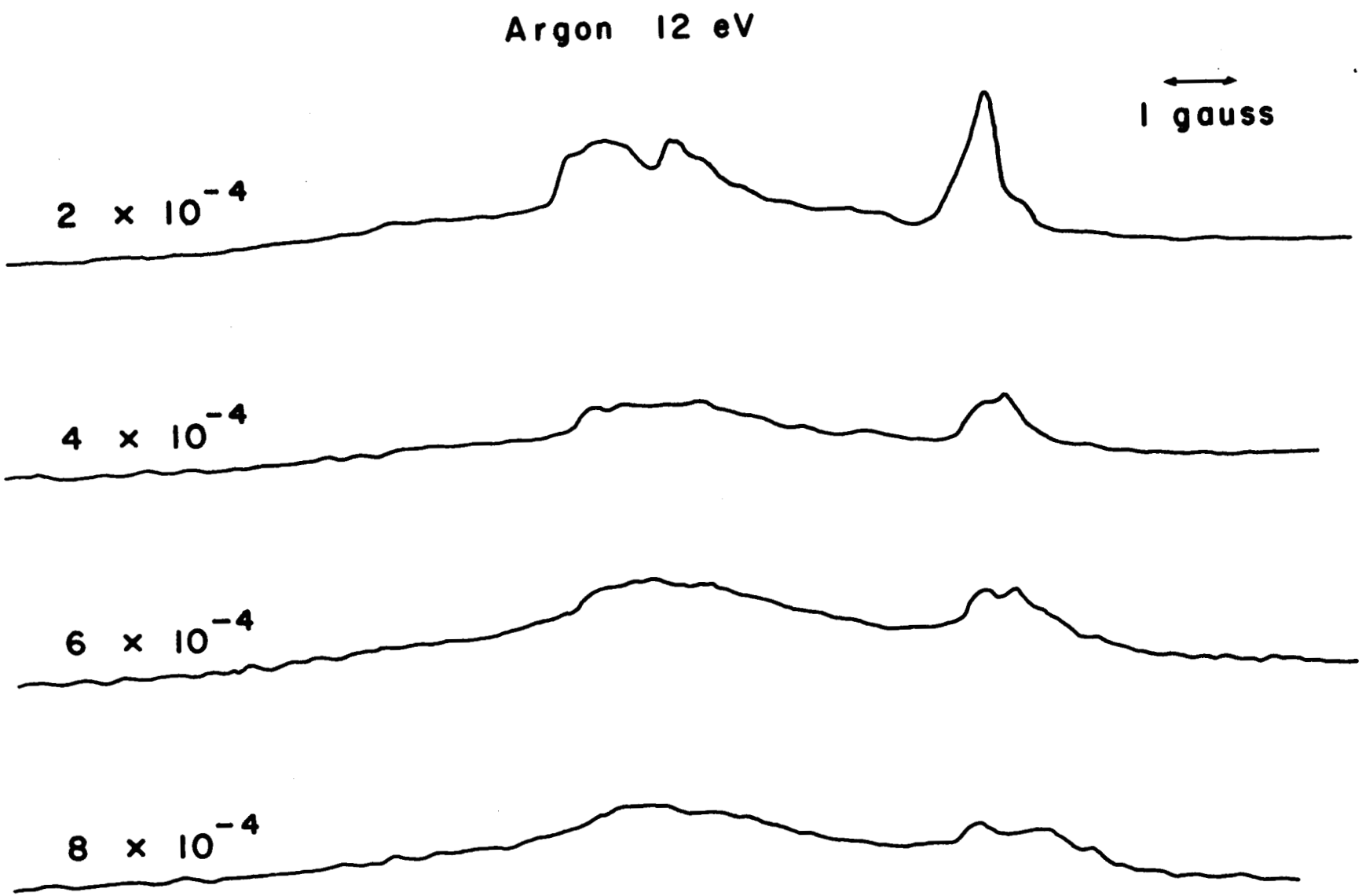

Fig. 17. Cyclotron resonance absorption spectra for 12 eV electrons in Argon.

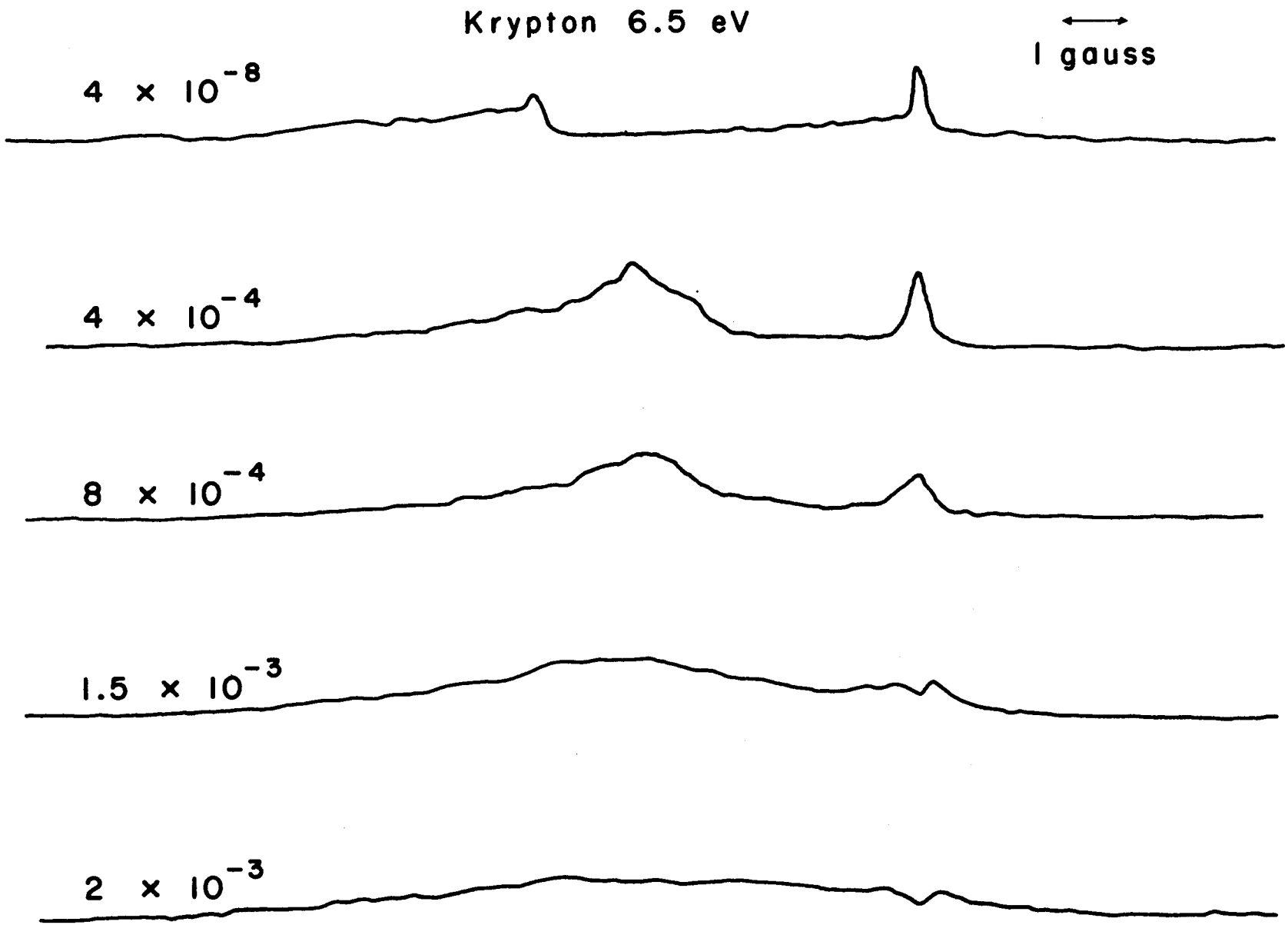

Fig. 18. Cyclotron resonance absorption spectra for 6.5 eV electrons in Krypton.

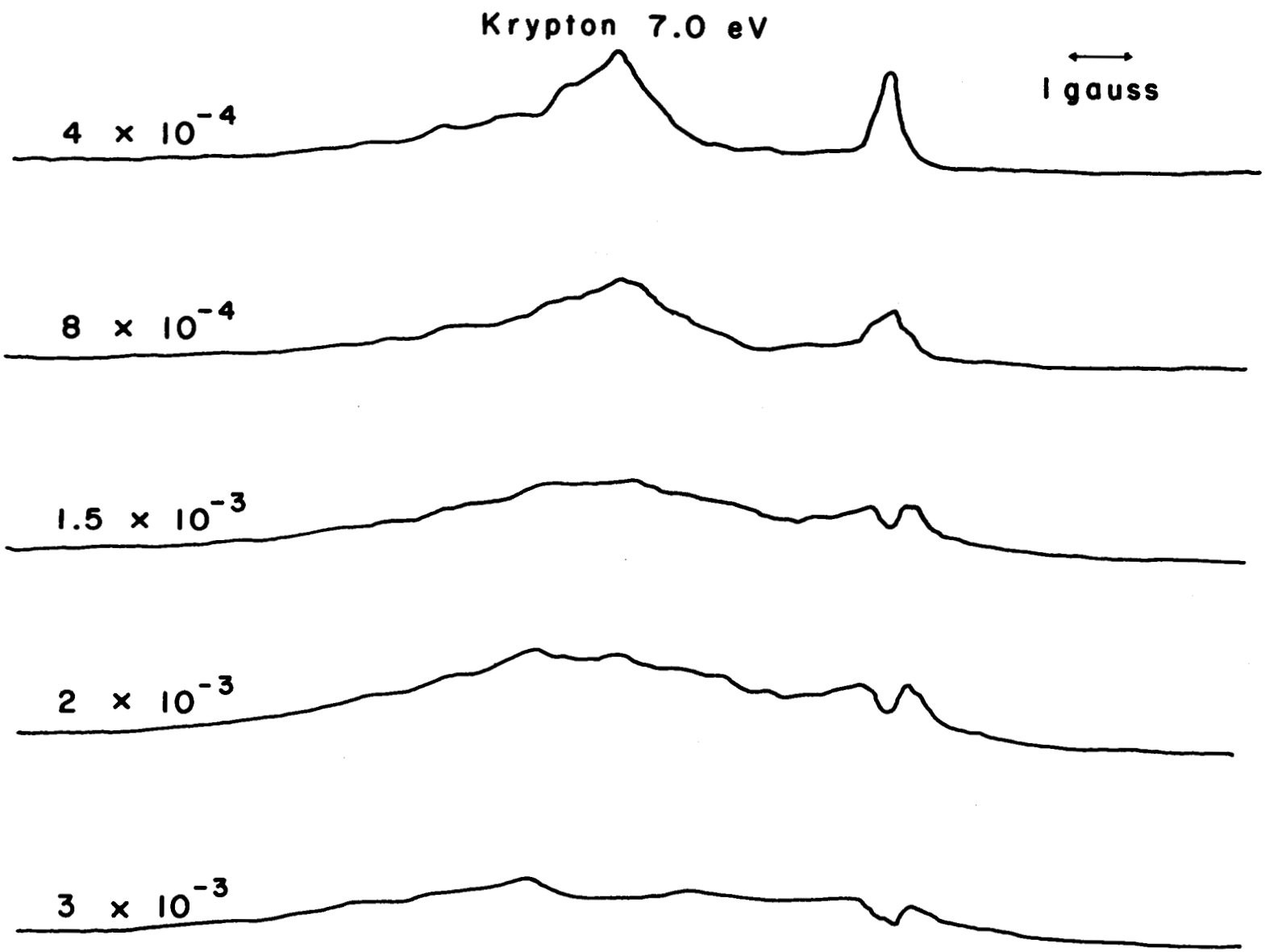

Fig. 19. Cyclotron resonance absorption spectra for 7 eV electrons in Krypton.

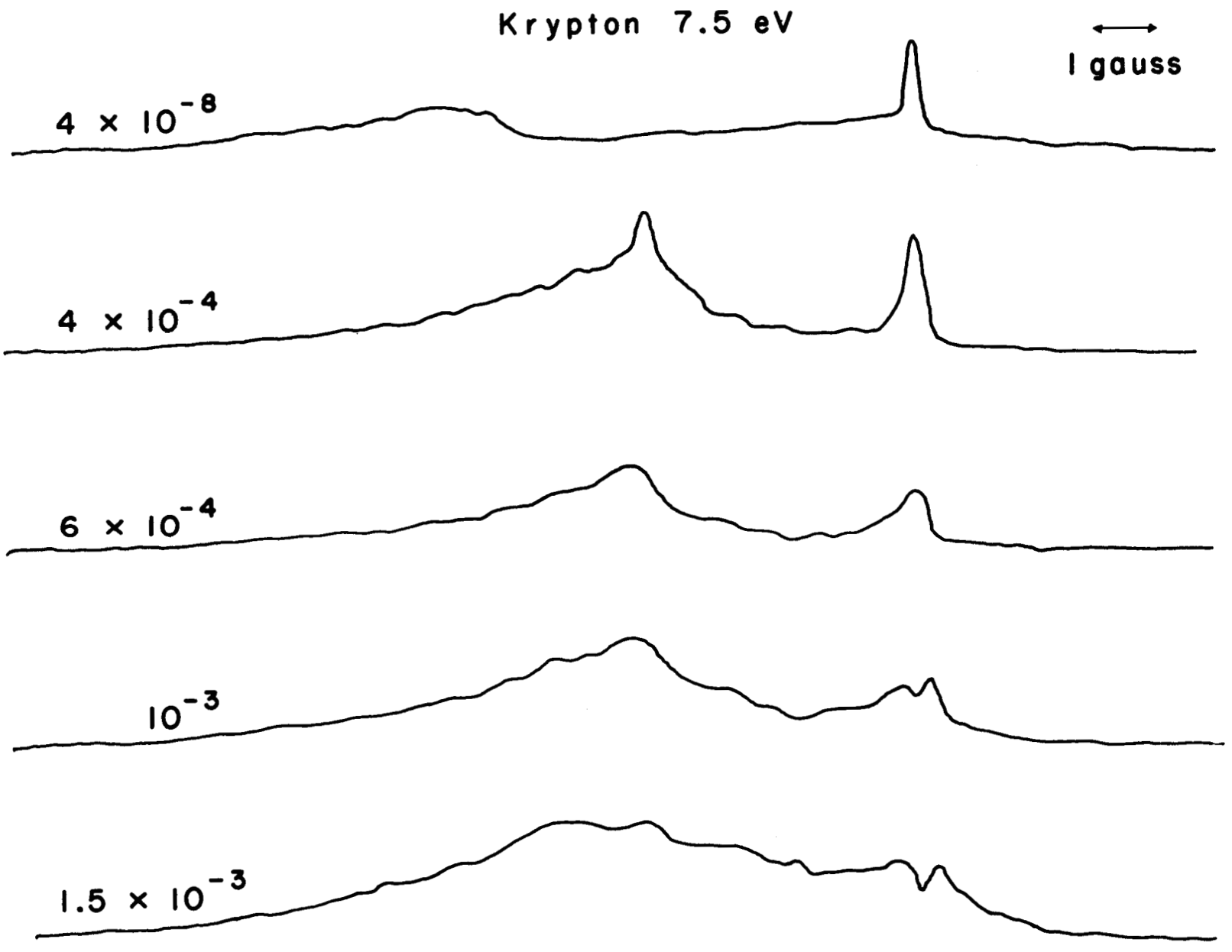

Fig. 20. Cyclotron resonance absorption spectra for 7.5 eV electrons in Krypton.

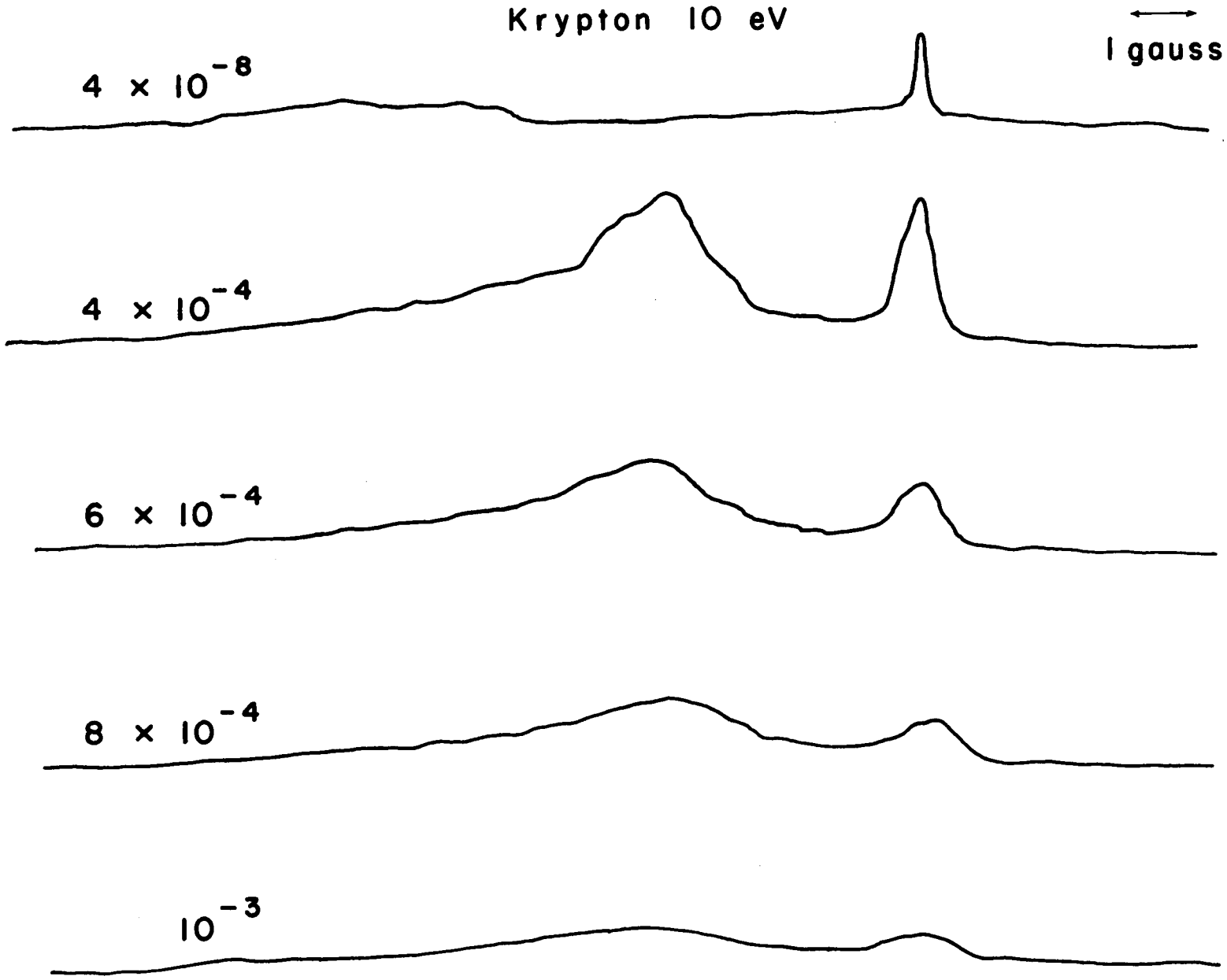

Fig. 21. Cyclotron resonance absorption spectra for 10 eV electrons in Krypton.

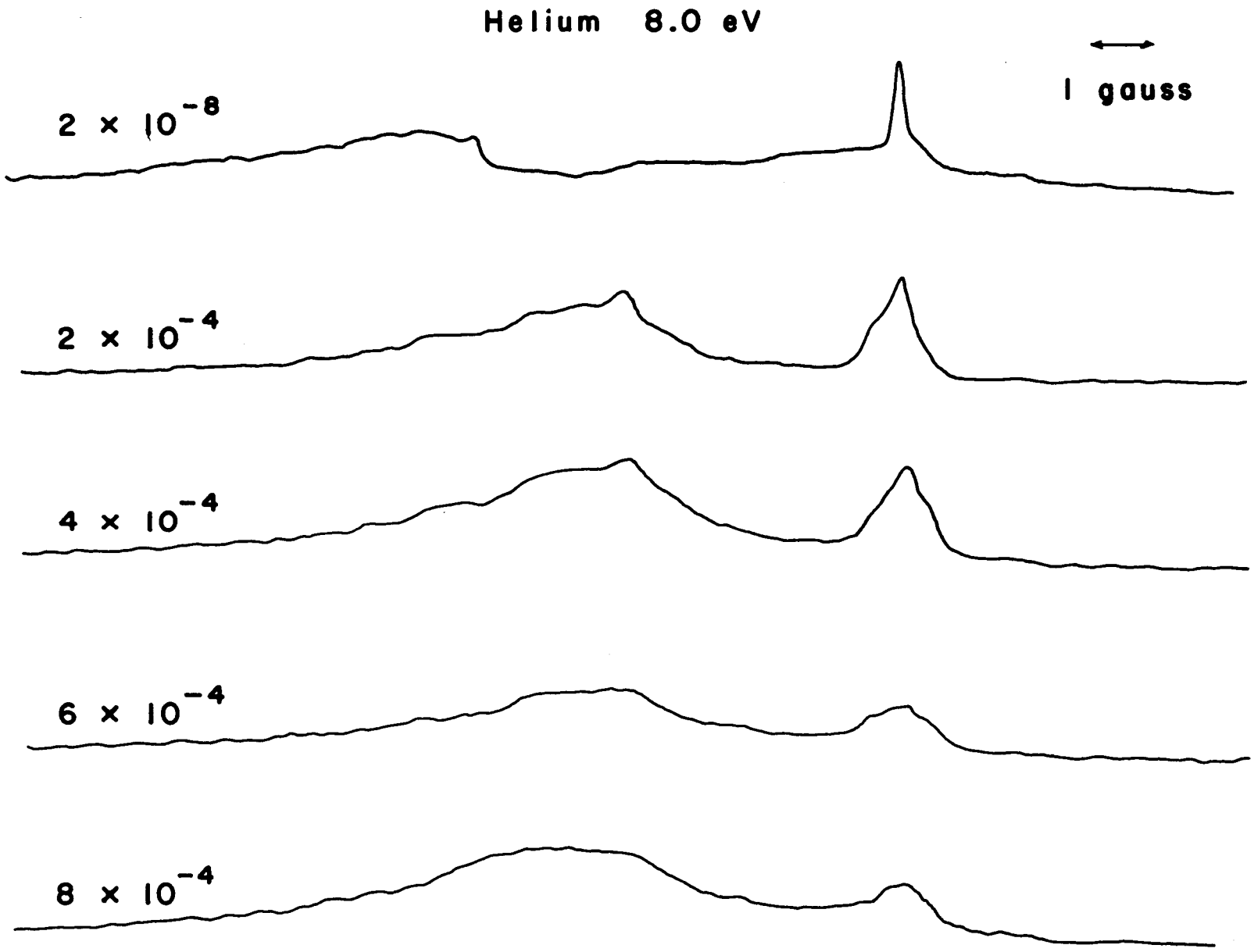

Fig. 22. Cyclotron resonance absorption spectra for 8 eV electrons in Helium.

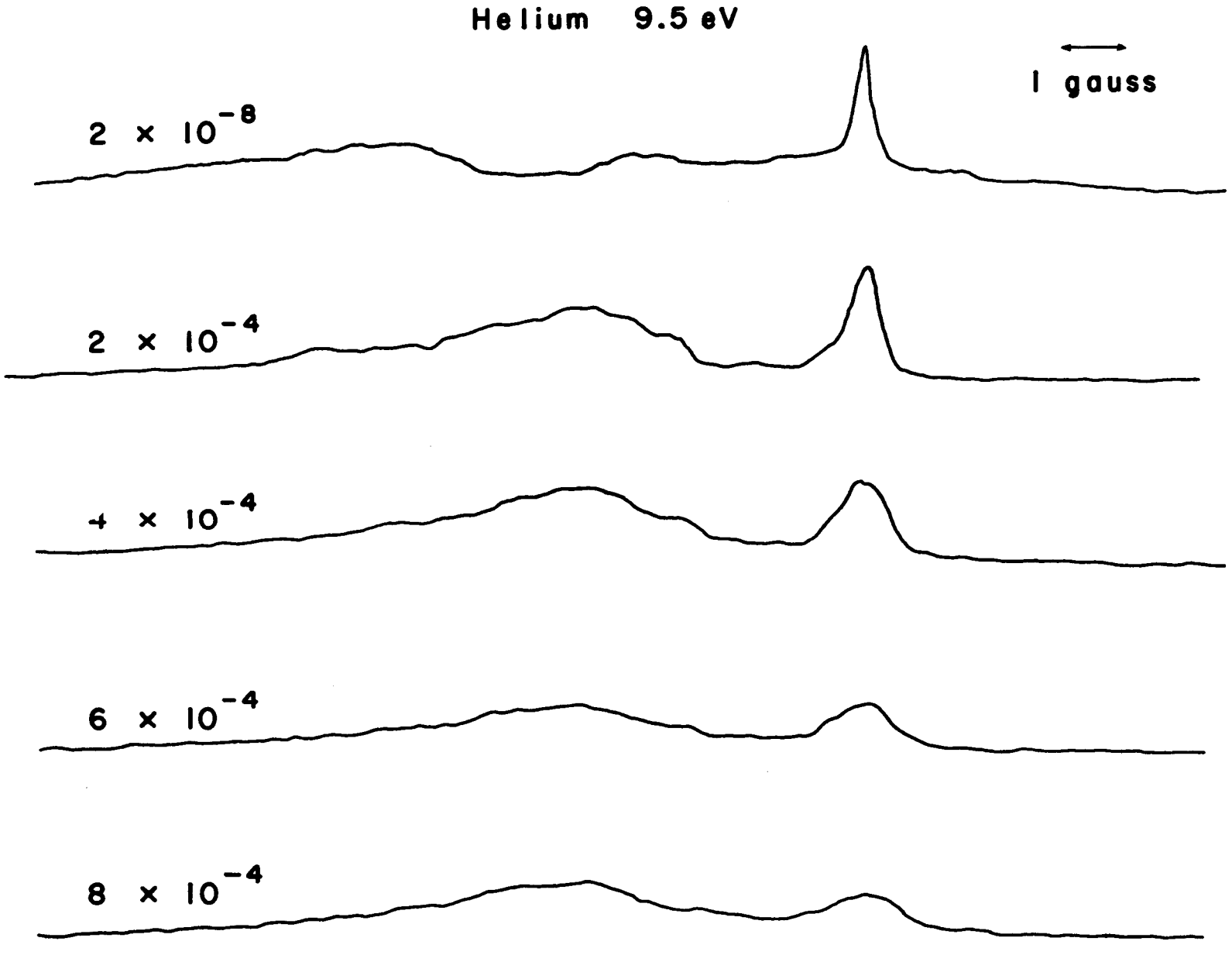

Fig 23. Cyclotron resonance absorption spectra for 9.5 eV electrons in Helium.

was in better agreement with estimates of the transit time broadening from drift energy measurements obtained with the second grid structure. In general, the average drift energy was between one fourth and one half of the total beam energy and the spread was moderately large. Fewer than 10 percent of the electrons in a given monoenergetic beam had less than 1 eV of drift energy or more than all but 1 eV of drift energy for the total beam energies represented in the data.

Referring to the data for Argon, the dip in the cyclotron resonance absorption line is observed to be progressively stronger in the spectra for 7 eV, 9 eV and 10 eV electrons. The Argon collision cross section for momentum transfer increases monotonically from the Ramsauer minimum until it levels off at about 12 eV. Only a slight suggestion of the dip appears in the data for 12 eV electrons in Argon.

The relative depth of the dip increased with pressure as it should have up to the point that collisions were the dominant broadening mechanism. At sufficiently high pressures the time that an electron spent in the cavity did not determine the width of the cyclotron resonance line. As the pressure was increased, the beam current was concurrently reduced from its approximately 1 microampere value in vacuum by scattering of the electrons along their long drift path from the cathode. An upper practical limit to the background gas pressure was thus reached at about 10^{-3} mm Hg depending upon the gas used.

The behavior of the cyclotron resonance absorption lineshape for Krypton was entirely similar except for the fact that the dip

disappeared completely at 10 eV. The cross section for Krypton levels off at about that energy. Measurements made with a background of Helium at electron gun potentials of 8 volts and 9.5 volts exhibit no dip at all. In this energy range the cross section for Helium is inversely proportional to the electron velocity and the collision frequency is, therefore, constant. The momentum transfer cross section information was obtained from the work of Frost and Phelps[32] who have combined and compared the measurements of many workers.

At this point the persistent occurence of the broad absorption at lower values of B_o than the absorption line identified as due to the cyclotron resonance interaction should be discussed. However, no explanation of its origin is available and it would be premature if not impossible to argue in favor of any speculative guesses. Within the context of this presentation its existence is noted and the contention that it does not alter the identification of the cyclotron resonance absorption is made.

3. Calculation of the Cyclotron Resonance Absorption Spectrum

From the foregoing remarks it appears that two parameters determine the shape of the cyclotron resonance absorption measured in these experiments. The first would be analogous to the single parameter $\alpha = P\nu_c'(P)/\nu_c(P)$ involved in the infinite plane wave analysis of chapter I. The second would express the number of collisions that an electron might be expected to suffer during the time it spent in the cavity. Two such parameters evolve from an analysis like the one offered in chapter II, section 5

for the case of relativistic electrons in vacuum.

For the present problem the linearized Boltzmann equation with the relaxational collision term is integrated along the unperturbed orbit of an electron as it traversed the cavity. The first order distribution function $f_1(\underline{p},\underline{r},t)$ is thus obtained and the field energy absorbed by the electron beam is calculated as indicated in Eq. (66). The fields are considered to be unperturbed by the presence of the electron beam and as in the calculation of chapter II, are assumed to be those of the empty resonator.

Since the electrons are non-relativistic the magnetic field of the cavity mode is neglected. The electric field is assumed to have a simpler spatial dependence than the actual zeroth order Bessel function variation of the electric field of the TM010 mode. It is assumed to oscillate with constant amplitude at all points on the electron beam subtended by the cavity, to vanish at points outside the length L subtended by the cavity and to lie along the $\hat{e}_y$ direction. The magnetic field $\underline{B}_o$ is parallel to $\hat{e}_z$ and the unperturbed orbits are once again given by Eqs. (60).

The linearized Boltzmann equation thus becomes

$$\frac{\partial f_1}{\partial t} + v_{\parallel} \frac{\partial f_1}{\partial z} - \Omega_o \frac{\partial f_1}{\partial \varphi} + \nu_c f_1 = - eE_1 \frac{\partial f_o}{\partial p_{\perp}} \sin \varphi \cos \omega t \ . \qquad (99)$$

The arguments that precede Eq. (58) also apply to the development of Eq. (99). Noting the parametrization of the unperturbed orbits in Eqs. (60) and the result in Eq. (61), the solution to Eq. (99) is seen to be

$$f_1(z,\underline{p},t) = - eE_1 \frac{\partial f_o}{\partial p_\perp} e^{-\nu_c t} \int_{-z/v_\parallel}^{o} d\tau \sin(\varphi-\Omega_o\tau) \cos \omega(t+\tau) e^{\nu_c(t+\tau)} . \tag{100}$$

Defining n as the electron density of the beam whose cross sectional area is σ, the average rate of field energy absorption by the electron beam is, according to Eq. (66),

$$\mathbb{P} = \frac{ne^2 E_1^{\,2} \pi\sigma L}{4} \int_o^\infty \frac{dp_\parallel}{p_\parallel} \int_o^\infty p_\perp dp_\perp \, f_o(p_\perp, p_\parallel) \, H \quad . \tag{101}$$

The absorption spectrum for a single value of $p_\perp$ and a single value of $p_\parallel$ is

$$H(x) = \left\{ \frac{\eta(2+\alpha)}{x^2+\eta^2} + \frac{2(x^2-\eta^2)-2\alpha\eta^2(1-\eta)}{(x^2+\eta^2)^2} \right.$$

$$+ (e^{-\eta}) \frac{[(\eta^2-x^2)\cos x - 2\eta x \sin x][2-\eta\alpha]+2\eta\alpha[\eta\cos x - x \sin x]}{(x^2+\eta^2)^2}$$

$$\left. + \frac{4\eta^2\alpha(\eta^2-x^2)}{(\eta^2+x^2)^3} - (4e^{-\eta}) \frac{\eta^2\alpha[(\eta^2-x^2)\cos x - 2\eta x \sin x]}{(\eta^2+x^2)^3} \right\} \tag{102}$$

where

$$\eta = \frac{\nu_c L}{v_\parallel} \tag{103}$$

$$\alpha = \frac{\nu_c'(p)}{\nu_c(p)} \frac{p_\perp^{\,2}}{p} \tag{104}$$

and

$$x = \frac{(\omega+\Omega_0)L}{v_{\parallel}} \quad . \tag{105}$$

The absorption spectrum $H(x)$ possesses the following properties:

1. It exhibits the dip at cyclotron resonance.
2. It reduces to the Lorentzian type line shape when collisions dominate over transit time effects.
3. In the absence of collisions it reduces simply to $\sin^2(x/2)/(x/2)^2$.

In conclusion it is noted that the condition for the onset of negative absorption at cyclotron resonance is

$$2 - \alpha - \frac{2}{\eta} + \frac{2\alpha}{\eta} + e^{-\eta}\left(\frac{2}{\eta} - \alpha - \frac{2\alpha}{\eta}\right) = 0 \tag{106}$$

which can be solved for η if $\alpha \geq 2$.

References

1. R. Q. Twiss, Australian J. Phys. 11, 564 (1958).
2. G. Bekefi, J. L. Hirshfield and S. C. Brown, Phys. of Fluids 4, 173 (1961).
3. I. B. Bernstein, Phys. Rev. 109, 10 (1958).
4. T. H. Stix, The Theory of Plasma Waves (McGraw-Hill Book Company, New York, 1962).
5. D. C. Montgomery and D. A. Tidman, Plasma Kinetic Theory (McGraw-Hill Book Company, New York, 1964).
6. E. S. Weibel, Phys. Rev. Lett. 2, 83 (1959).
7. E. G. Harris, J. Nucl. Energy, Part C, 2, 138 (1961).
8. E. P. Gross, Phys. Rev. 82, 232 (1951).
9. H. Weitzner, Phys. of Fluids 6, 1123 (1963).
10. L. Landau, J. Physics U.S.S.R. 10, 25 (1946).
11. I. B. Bernstein, S. K. Trehan and M. P. H. Weenink, Nuclear Fusion 4, 61 (1964).
12. G. Bekefi, Radiation Processes in Plasma (John Wiley and Sons, New York, 1966).
13. Y. Terumichi, T. Idehara, I. Takahashi, H. Kubo and K. Mitani, J. Phys. Soc. Japan 20, 1705 (1965).
14. P. L. Bhatnagar, E. P. Gross and M. Krook, Phys. Rev. 94, 511 (1954).
15. R. B. Brode, Rev. Mod. Phys. 5, 257 (1933).
16. R. Wingerson, Phys. Rev. Lett. 6, 446 (1961).
17. H. Dreicer, H. J. Karr, E. A. Knapp, J. A. Phillips, E. J. Stovall Jr. and J. L. Tuck, Nuclear Fusion, Supplement, Part I, 299 (1962).

18. H. Karr, E. Knapp and W. Riesenfeld, Phys. of Fluids, 6, 501 (1963).

19. T. G. Northrop, The Adiabatic Motion of Charged Particles (Interscience Publishers, Inc., New York, 1963).

20. S. Chandrasekhar, Plasma Physics (University of Chicago Press, Chicago, 1960).

21. F. Rosebury, Handbook of Electron Tube and Vacuum Techniques (Addison-Wesley Publishing Co., Reading, Mass., 1965).

22. N. Bloembergen, E. M. Purcell and R. V. Pound, Phys. Rev. 73, 679 (1948).

23. J. P. Gordon, Rev. of Scientific Instruments 32, 658 (1961).

24. J. E. Drummond, Phys. Rev. 110, 293 (1958).

25. J. D. Jackson, Classical Electrodynamics (John Wiley and Sons, New York, 1962), pp. 468-472.

26. H. Goldstein, Classical Mechanics (Addison-Wesley Publishing Company, Reading, Mass., 1959), pp. 266-268.

27. E. H. Kennard, Kinetic Theory of Gases (McGraw-Hill Book Company, New York, 1938).

28. E. A. Desloge and S. W. Matthysse, Am. J. Phys. 28, 1 (1960).

29. S. Tanaka and K. Mitani, J. Phys. Soc. Japan 19, 1376 (1964).

30. Y. Terumichi, T. Idehara, S. Takahashi, H. Kubo and K. Mitani, J. Phys. Soc. Japan 19, 1993 (1964).

31. H. Fields, G. Bekefi and S. C. Brown, Phys. Rev. 129, 506 (1963).

32. L. S. Frost and A. V. Phelps, Phys. Rev. 136, 1538 (1964).